

Supporting Information

Facile synthesis of nitroamino-1,3,4-oxadiazole with azo linkage: a new family of high-performance and biosafe energetic materials

Shreyasi Banik,^{a†} Pradeep Kumar,^{a†} Vikas D. Ghule,^b Shweta Khanna,^c Dharmaraja Allimuthu,^c and Srinivas Dharavath^{*a}

a. Energetic Materials Laboratory, Department of Chemistry, Indian Institute of Technology Kanpur, Kanpur-208016, Uttar Pradesh, India. E-mail: srinivasd@iitk.ac.in

b. Department of Chemistry, National Institute of Technology Kurukshetra, Kurukshetra-136119, Haryana, India.

c. Chemical Biology Laboratory, Department of Chemistry, Indian Institute of Technology Kanpur, Kanpur-208016, Uttar Pradesh, India.

Table of Contents

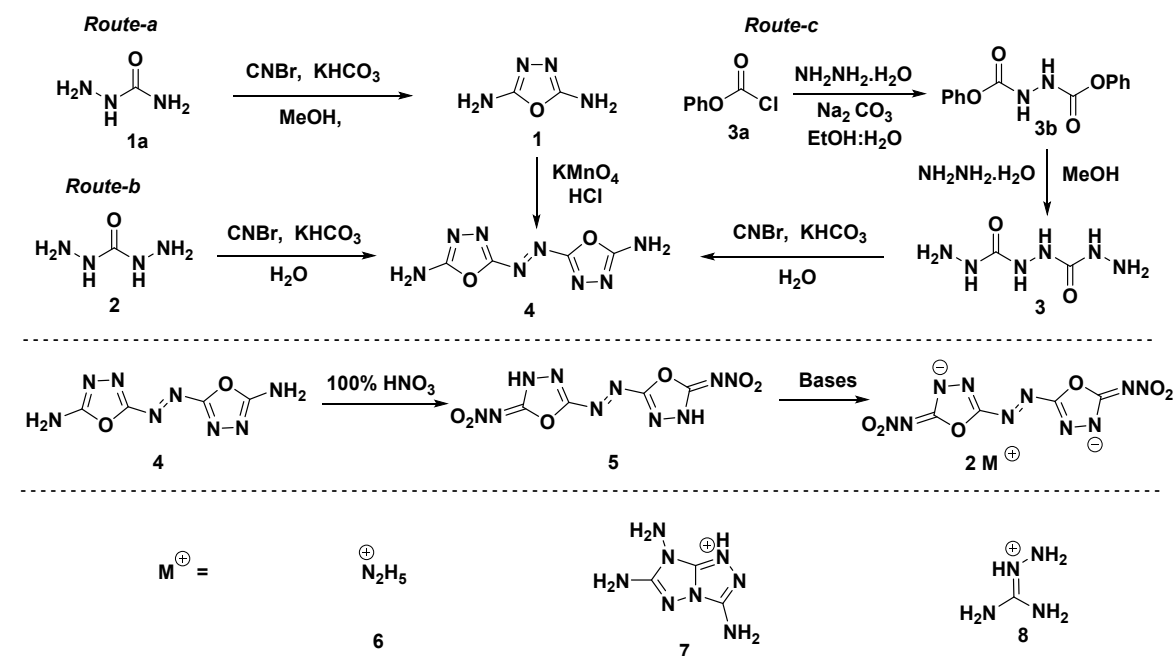
Entry	Page No
General Methods and plausible synthetic mechanism of 5	2-9
Crystal Structure Analysis for 4 , 5 and 9	9-27
Resazurin-based cell viability assay for compounds.	28
NMR, Mass Spectra for 1	29-30
NMR spectra for 3b	30-31
NMR Spectra for 3	32
NMR, IR, Mass Spectra, DSC plots, and TGA curve for 4	33-35
NMR, IR, Mass Spectra, DSC plots, and TGA curve for 5.2H₂O	36-38
NMR, IR, DSC plots, and TGA curve for 6	39-41
NMR, IR, DSC plots, and TGA curve for 7	41-44
NMR, IR, DSC plots, and TGA curve for 8	45-47
Computational Details	49-54
Thermal Studies of 7 using Kissinger method	55-59
Non-Covalent Interaction graph	60-62
References	62-63

Experimental Procedures

Caution! The compounds in this work are energetic materials that could potentially explode under certain conditions (e.g., impact, friction, or electric discharge). Appropriate safety precautions, such as the use of shields in a fume hood and personal protection equipment (safety glasses, face shields, earplugs, as well as gloves) should be always taken when handling these materials.

General. All reagents were purchased from AKSci or TCI or Merck in analytical grade and were used as supplied. ^1H NMR and ^{13}C NMR, ^{15}N NMR spectra were recorded in JEOL DELTA (ECS) 500 (^1H , 500 MHz; ^{13}C , 126 MHz) nuclear magnetic resonance spectrometer. Chemical shifts for ^1H NMR, ^{13}C NMR, and ^{15}N spectra are given concerning external $(\text{CH}_3)_4\text{Si}$ (^1H and ^{13}C) and CH_3NO_2 (^{15}N). [d6] DMSO was used as a locking solvent unless otherwise stated. IR spectra were recorded using Zn-Se crystal with an ECO-ATR spectrometer (Bruker Alpha II). Density was determined at room temperature by employing Anton Par Ultra5000 gas pycnometer. Decomposition temperatures (onset) were recorded using a dry nitrogen gas purge and a heating rate of $5\text{ }^\circ\text{C min}^{-1}$ on a differential scanning calorimeter (DSC, Mettler). HRMS was recorded on a Quadrupole Time-of-Flight Mass Spectrometry mass spectrometer and ESI-MS was recorded on Agilent mass spectrometer. Impact and friction sensitivity measurements were made using a standard BAM fall hammer and a BAM friction tester.

General Synthetic Route

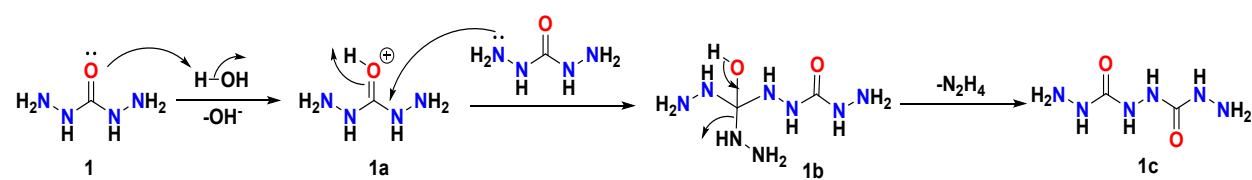


Scheme 1: Synthesis of (E)-5,5'-(diazene-1,2-diyl)bis(1,3,4-oxadiazol-2-amine) (**4**), (E)-N,N'-(diazene-1,2-diylbis(1,3,4-oxadiazole-5,2-diyl))dinitramide (**5**) and its salts (**6-8**).

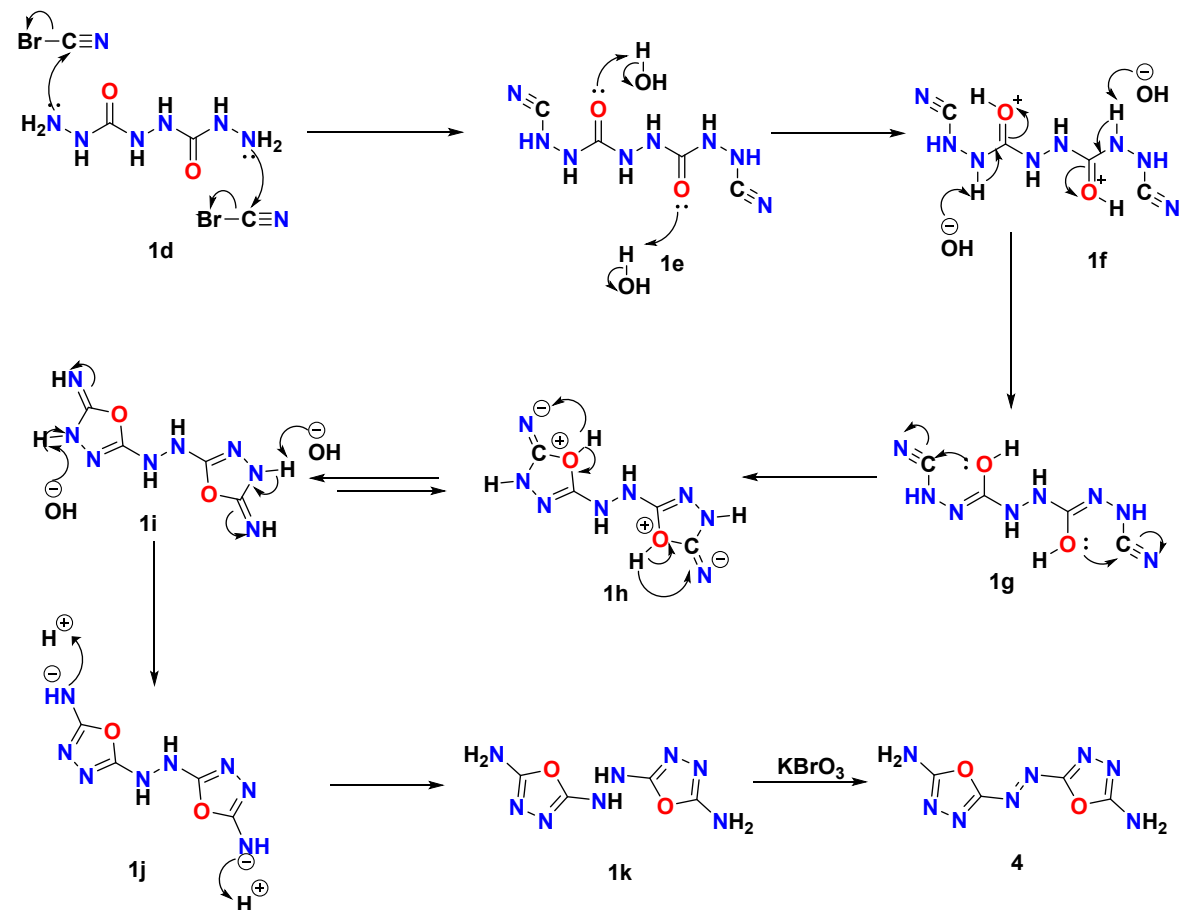
Plausible reaction mechanism demonstrated below.

Carbohydrazide was dissolved in water and stirred until it is completely getting solubilized.

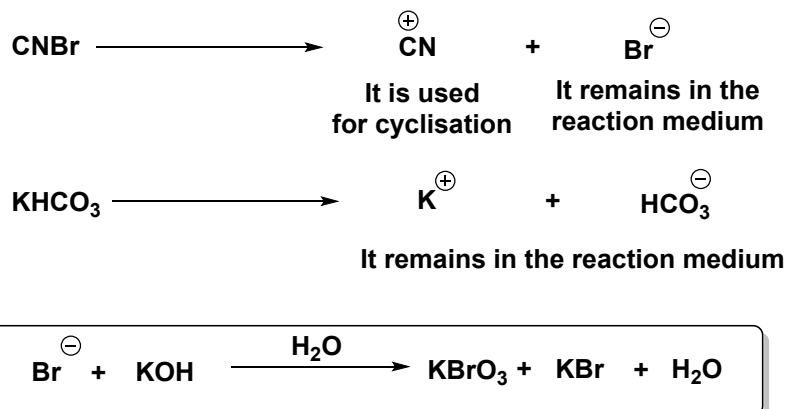
The compound dimerizes to form **1c** (which is also formed during Route C synthesis from phenyl chloroformate and hydrazine hydrate). After 2 hours, KHCO_3 was added in the reaction mix. In the reaction mix KBrO_3 (very powerful oxidizing agent) is generated in situ via the following mechanism, which helps to oxidise **1k** to form **4**



Route B and C: Further, CNBr addition to the reaction mix causes cyclization to form 1,3,4-oxadiazole with NH-NH bridge (**1k**).



In situ oxidiser (KBrO_3) formation in the reaction medium



KBrO_3 is a strong oxidizing agent. It is also used as a source of Br_2 in presence of Br^- .

Ref:

1. Electrochemical and Solid-State Letters, 13 11H385-H387 2010
2. Johnson Matthey Technol. Rev., 2019, 63, (1)

Route a:



Synthesis of 1,3,4-oxadiazole- 2,5-diamine (1): Semicarbazide (**1a**) (2.25 g, 30 mmol) was dissolved in methanol (15 ml) and cyanogen bromide (3.15 g, 30 mmol) was added at 25 °C. Then the suspension was stirred for 16 hrs at same temperature. The formed precipitate was collected by filtration and the solvent was removed by rotatory evaporated to afford a white solid 1,3,4-oxadiazole- 2,5-diamine (**1**) with 90 % yield (2.7 g, 27 mmol). ^1H (DMSO-d6): δ = 8.39 (s, 4H); ^{13}C (DMSO-d6): δ = 156.0. HRMS (ESI) m/z (M+H) $^+$ Calculated for $\text{C}_2\text{H}_5\text{N}_4\text{O}^+$: 101.0458. Found: 101.0456.



Synthesis of (E)-5,5'-(diazene-1,2-diyl)bis(1,3,4-oxadiazol-2-amine) (4): Compound **1** (1.00 g, 10 mmol) was dissolved in 25 mL of 37% HCl, potassium permanganate (1.98 g, 25 mmol) was taken in 25 mL of water and slowly added to compound **1** at 25 °C. The reaction mixture was stirred at 50 °C for 8 hrs and cooled to room temperature. Formed red colour precipitate of **4** was collected by filtration with 20 % yield (0.392 g, 2 mmol). T_d (onset): 240 °C. ^1H (DMSO-d6): δ = 8.31 (s, 4H) ppm; ^{13}C (DMSO-d6): δ = 164.18, 163.54; IR (ATR ZnSe): 3324(w), 3048(w), 1662(s), 1567(m), 1515(w), 1407(m), 1295(w), 1071(s), 965(m), 811(w), 736(w), 678(m) cm^{-1} . HRMS (ESI) m/z (M+H) $^+$ Calculated for $\text{C}_4\text{H}_5\text{N}_8\text{O}_2^+$: 197.0530. Found: 197.0525. Elemental analysis calculated (%) for $\text{C}_4\text{H}_4\text{N}_8\text{O}_2 \cdot \text{H}_2\text{O}$ (205.05): C (22.44), H (2.82), N (52.33); found: C (23.38), H (2.50), N (52.42).

Route b:

Carbohydrazide (**2**) (0.9 g, 10 mmol) was dissolved in water (10 ml) and stirred until get solubilized. Cyanogen bromide (2.11 g, 20 mmol) was added to it at 25 °C and the red-coloured precipitate was observed after 30 minutes. The formed suspension was stirred for 2 hrs at same temperature and potassium bicarbonate (2.00 g, 20 mmol) was added portion wise. The reaction mixture was stirred for another 2 hrs at same temperature. Formed precipitate was collected by filtration and washed with water (2*10 mL) and methanol (2*10 mL). The precipitate was dried to afford compound **4** in 35% yield (0.686 g, 3.5 mmol).

Route c:



Synthesis of Diphenyl hydrazodicarboxylate (3b): In the round bottom flask, sodium carbonate (2.55 g, 25 mol) was taken in 50:50% mixture of ethanol and water (12.5 ml each), hydrazine monohydrate (1.21 ml, 0.025 mol) was added to it. After few minutes, phenyl chloroformate (6.27 ml, 0.05 mol) was added dropwise using an addition funnel and left to stir at 25 °C. After 1 hr of stirring at same temperature, white precipitate was observed, which was filtered, washed with ethanol, and dried to give the desired white compound (**3b**) 95 % yield (6.46 g, 23.7 mmol). ^1H (DMSO-d6): δ = 9.95(s, 2H), 7.42(t, J = 10 Hz), 7.25 (t, J = 10 Hz), 7.14(d, J = 10 Hz); ^{13}C (DMSO-d6): δ = 154.75, 150.52, 129.50, 125.50, 121.47.



Synthesis of N, N'-Dicarbazoylhydrazine (3): 50% Hydrazine monohydrate (6.0 ml, 18.75 mmol) was added dropwise to the solution of diphenyl hydrazodicarboxylate (**3b**) (5.0 g, 18.38 mmol) in methanol (30 ml). The mixture was stirred at 25 °C for 12 hrs. The formed off-white precipitate was filtered, washed with methanol (10 ml), diethyl ether (10 ml), and dried under reduced pressure to give white solid **3** in 94 % yield (2.60 g, 17.62 mmol). ¹H (DMSO-d6): δ = 7.73(s, 2H), 7.32(s, 2H), 4.02(s, 4H); ¹³C (D₂O): δ = 161.81.

Synthesis of (E)-5,5'-(diazene-1,2-diyl)bis(1,3,4-oxadiazol-2-amine) (4): N, N'-Dicarbazoylhydrazine (**3**) (1.48 g, 10 mmol) was dissolved in water (15 ml), cyanogen bromide (2.12 g, 20 mmol) was added to it at room temperature. The red-colored precipitate was observed after 30 minutes and the same was stirred for 3 hrs. Potassium bicarbonate (2.20 g, 22 mmol) was added by portions and stirred for 4 more hours at the same temperature. The formed red solid was collected by filtration and washed with water and methanol to afford compound **4** in 90 % yield (1.76 g, 9 mmol).

Table S1: Optimization table for the synthesis of compound (4) *route-c*:

Entry	Solvent	Additive (eq.) added after-h	T (°C)	Time (hrs)	Yield (%)
1	Methanol	-	25	24	NA
2	Ethanol	-	25	24	NA
3	Ethanol	-	50	24	NA
4	Ethanol	-	50	24	10 ^a
5	Ethanol+H ₂ O (1:1)	-	25	24	20 ^a
6	H ₂ O	-	25	24	34 ^a
7	H ₂ O	KHCO ₃ (2.0)-0 h	25	12	55 ^a
8	H ₂ O	KHCO ₃ (2.0)-4 h	25	12	65 ^a
9	H ₂ O	KHCO ₃ (2.0)-3 h	25	12	84 ^a
10	H ₂ O	KHCO ₃ (2.0)-2 h	25	12	70 ^a
11	H ₂ O	KHCO ₃ (2.0)-3 h	50	12	70 ^a

12	H ₂ O	KHCO ₃ (2.0)-3 h	25	7	90 ^a
----	------------------	-----------------------------	----	---	-----------------

In all reactions, CNBr was used 2.0 equivalent, Yield-Isolated yields. (a) Reaction was done in open air.



Synthesis of 5,5'-(E)-diazene-1,2-diylbis(2-(nitroimino)-1,3,4-oxadiazole (5.2H₂O): Compound **4** (1 g, 5.10 mmol) was added by portions into stirred 100% HNO₃ (10 ml) at 0 °C, reaction was continued at same temperature for 24 hrs and poured into crushed ice (10 g). The formed precipitate was collected by filtration and washed with cold water, dried in air to afford yellow coloured compound **5** in 82 % yield (1.19 g, 4.16 mmol). T_d (onset): 183 °C. ¹H (DMSO-d6): δ = 9.93 (br, s, 2H) ppm; ¹³C (DMSO-d6): δ = 163.43, 161.75; IR (ATR ZnSe): 3740(w), 3320(w), 1653(s), 1523(s), 1401(s), 1316(s), 1146(m), 1056(s), 995(s), 899(w), 748(m), 676(m) cm⁻¹. HRMS (ESI) m/z (M+H)⁺ calculated for C₄H₂N₁₀O₆: 287.0232. Found: 287.0444. Elemental analysis calculated (%) for C₄H₂N₁₀O₆·0.5H₂O (286.01): C (16.28), H (1.02), N (47.46); found: C (16.86), H (0.60), N (47.48).

Table S2: Optimization table for the synthesis of compound (**5**)

Entry	Nitrating reagents	T (°C)	Amount of HNO ₃ (mL)	Time (hrs)	Yield (%)
1	100% HNO ₃	25	2 mL ^a	2	NA
2	100% HNO ₃	25	2 mL ^a	4	NA
3	100% HNO ₃	25	2 mL ^a	6	NA
4	100% HNO ₃	25	5 mL ^b	12	15
5	100% HNO ₃	25	5 mL ^b	24	47
6	100% HNO ₃	0	5 mL ^b	24	78
7	100% HNO ₃	25	10 mL ^c	24	54
8	100% HNO ₃	0	10 mL ^c	24	82

In all the reaction conditions, pinch by pinch addition of substrate in the nitrating mixture was done at 0 °C in the ice bath a: 200 mg substrate was taken; b: 500 mg substrate was taken; c: 1 gram substrate was taken

General Procedure for the Synthesis of the Salts 6–8

5,5'-(*(E)*-diazene-1,2-diyl)bis(2-(nitroimino)-1,3,4-oxadiazole (**5**) (0.286 g, 1 mmol) was dissolved in 5 mL of methanol, added, hydrazine monohydrate (0.064 mL, 2 mmol), 3,6,7-Triamino-7H-[1,2,4]triazolo[4,3-b][1,2,4]triazole (TATOT) (0.308 g, 2 mmol), aminoguanidine hydrochloride (0.22 g, 2 mmol), and aqueous ammonia (0.046 mL, 2 mmol) to it and reaction mixtures were stirred for 1 hr at room temperature. The formed precipitate was collected by filtration, and dried in air to afford desired products **6–9** in quantitative yields.



Hydrazine salt of 5,5'-(*(E)*-diazene-1,2-diyl)bis(2-(nitroimino)-1,3,4-oxadiazole (6): Yield: 93 % (0.327 g, 0.92 mmol). Td (onset): 143 °C. ^1H (DMSO-d6): δ = 7.24 (br, s, 10H) ppm; ^{13}C (DMSO-d6): δ = 165.80, 164.24; IR(ATR ZnSe): 3304(w), 1500(s), 1420(m), 1290(s), 1238(m), 1090(m), 978(m) cm^{-1} . Elemental analysis calculated (%) for $\text{C}_{4}\text{H}_{10}\text{N}_{14}\text{O}_6 \cdot 0.5\text{CH}_3\text{OH} \cdot \text{H}_2\text{O}$ (352.10): C (14.07), H (3.67), N (51.03); found: C (13.59), H (3.08), N (51.10).



3,6,7-triamino-7H-[1,2,4]triazolo[4,3-b][1,2,4]triazole salt of 5,5'-(*(E)*-diazene-1,2-diyl)bis(2-(nitroimino)-1,3,4-oxadiazole (7): Yield: 94 % (0.560 g, 0.94 mmol). Td (onset): 228 °C. ^1H (DMSO-d6): δ = 8.20 (s, 2H), 7.23 (s, 2H), 5.77 (s, 2H) ppm; ^{13}C (DMSO-d6): δ = 165.76, 164.32, 160.13, 147.41, 141.10; IR(ATR ZnSe): 3393(w), 1659(s), 1501(s), 1446(m), 1274(s), 1235(s), 1092(s), 1034(m), 986(m), 852(m) cm^{-1} . Elemental analysis calculated (%) for $\text{C}_{10}\text{H}_{14}\text{N}_{26}\text{O}_6 \cdot \text{H}_2\text{O}$ (506.20): C (19.61), H (2.63), N (59.47); found: C (20.00), H (2.21), N (59.40).



Aminoguanidine salt of 5,5'-(*(E*)-diazene-1,2-diyl)bis(2-(nitroimino)-1,3,4-oxadiazole (8**):**
Yield: 94 % (0.409 g, 0.94 mmol). Td (onset): 181 °C. ^1H (DMSO-d6): δ = 8.55 (s, 1H), 7.24 (br, s, 2H), 6.71 (br, s, 2H), 4.67 (br, s, 2H) ppm; ^{13}C (DMSO-d6): δ = 165.76, 164.32, 158.73; IR(ATR ZnSe): 3468(w), 3363(w), 1664(s), 1502(s), 1415(w), 1291(s), 1236(m), 1084(m), 1032(w), 989(w) cm $^{-1}$. Elemental analysis calculated (%) for $\text{C}_6\text{H}_{14}\text{N}_{18}\text{O}_6$ (434.13): C (16.59), H (3.25), N (58.05); found: C (16.01), H (3.51), N (57.92).

Results and Discussion

X-Ray Crystal structure details

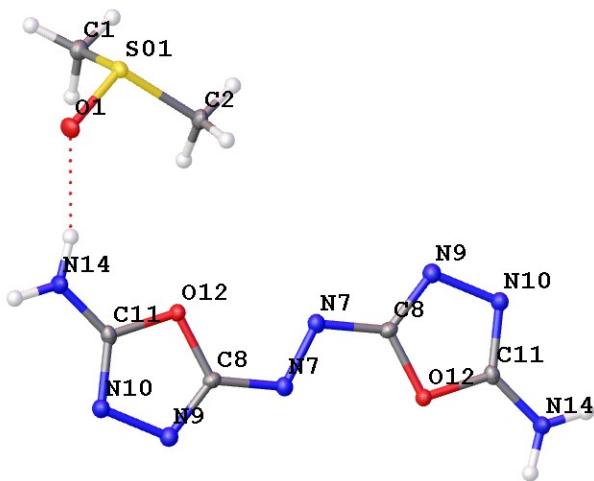


Figure S1: Molecular Structure of **4**.

Table S3 Crystal data and structure refinement for **4**.

CCDC No.	2173450
Empirical formula	$\text{C}_8\text{H}_{16}\text{N}_{18}\text{O}_4\text{S}_2$
Formula weight	352.41
Temperature/K	100
Crystal system	triclinic
Space group	P-1
a/Å	6.0576(8)
b/Å	7.4466(10)
c/Å	8.8862(13)
$\alpha/^\circ$	75.730(4)
$\beta/^\circ$	86.042(4)

$\gamma/^\circ$	77.998(4)
Volume/ \AA^3	379.92(9)
Z	1
$\rho_{\text{calc}} \text{g/cm}^3$	1.540
μ/mm^{-1}	0.382
F(000)	184.0
Crystal size/mm ³	0.33 × 0.33 × 0.22
Radiation	MoK α ($\lambda = 0.71073$)
2 Θ range for data collection/°	5.758 to 56.624
Index ranges	-8 ≤ h ≤ 8, -9 ≤ k ≤ 9, -11 ≤ l ≤ 11
Reflections collected	3954
Independent reflections	1853 [$R_{\text{int}} = 0.0298$, $R_{\text{sigma}} = 0.0386$]
Data/restraints/parameters	1853/0/102
Goodness-of-fit on F ²	1.111
Final R indexes [I>=2σ (I)]	$R_1 = 0.0319$, $wR_2 = 0.0721$
Final R indexes [all data]	$R_1 = 0.0343$, $wR_2 = 0.0734$
Largest diff. peak/hole / e \AA^{-3}	0.33/-0.38

Table S4 Fractional Atomic Coordinates ($\times 10^4$) and Equivalent Isotropic Displacement Parameters ($\text{\AA}^2 \times 10^3$) for 4. U_{eq} is defined as 1/3 of the trace of the orthogonalised U_{ij} tensor.

Atom	x	y	z	U(eq)
S01	7404.4(6)	1000.7(5)	1170.0(4)	11.49(11)
O12	3849.6(16)	3110.1(14)	5198.2(11)	12.0(2)
O1	8332.7(17)	203.5(15)	2800.4(12)	16.2(2)
N10	5281(2)	2680.7(17)	7548.0(14)	13.8(2)
N7	215(2)	4978.0(17)	5701.3(14)	12.4(2)
N9	3120(2)	3777.1(17)	7518.9(14)	13.9(2)
N14	7442(2)	1302.8(18)	5641.5(14)	15.8(3)
C11	5631(2)	2314.3(19)	6158.3(16)	11.7(3)
C8	2329(2)	3985.7(19)	6152.4(16)	11.8(3)
C1	8897(2)	2828(2)	265.8(17)	14.9(3)
C2	4734(2)	2468(2)	1416.3(17)	14.8(3)

Table S5 Anisotropic Displacement Parameters ($\text{\AA}^2 \times 10^3$) for 4. The Anisotropic displacement factor exponent takes the form: $-2\pi^2[h^2a^*{}^2U_{11} + 2hka^*b^*U_{12} + \dots]$.

Atom	U ₁₁	U ₂₂	U ₃₃	U ₂₃	U ₁₃	U ₁₂
S01	11.27(17)	11.88(17)	11.17(17)	-3.74(12)	-2.44(12)	-0.05(12)
O12	9.8(4)	14.1(5)	11.1(5)	-3.7(4)	-1.6(4)	0.8(4)
O1	15.1(5)	18.6(5)	11.8(5)	-2.3(4)	-5.3(4)	3.8(4)
N10	11.6(6)	16.4(6)	12.9(6)	-4.2(5)	-1.3(4)	-0.5(5)
N7	11.4(5)	13.2(5)	12.5(6)	-2.6(4)	-1.2(4)	-2.1(5)
N9	12.5(6)	14.7(6)	14.4(6)	-4.5(5)	-1.4(4)	-0.8(5)
N14	11.8(6)	21.5(6)	12.4(6)	-5.3(5)	-2.9(4)	3.0(5)
C11	10.5(6)	12.5(6)	11.4(6)	-0.7(5)	-2.5(5)	-2.3(5)
C8	11.4(6)	12.6(6)	11.5(6)	-4.4(5)	1.1(5)	-1.3(5)
C1	12.5(6)	17.0(7)	16.1(7)	-5.1(5)	0.2(5)	-3.8(6)
C2	9.5(6)	18.6(7)	14.0(7)	-2.1(5)	-1.5(5)	0.9(5)

Table S6 Bond Lengths for 4.

Atom	Atom	Length/ \AA	Atom	Atom	Length/ \AA
S01	O1	1.5223(10)	N10	C11	1.3230(18)
S01	C1	1.7851(15)	N7	N7 ¹	1.282(2)
S01	C2	1.7866(14)	N7	C8	1.3702(18)
O12	C11	1.3622(16)	N9	C8	1.2978(18)
O12	C8	1.3811(16)	N14	C11	1.3185(18)
N10	N9	1.3895(17)			

¹-X,1-Y,1-Z

Table S7 Bond Angles for 4.

Atom	Atom	Atom	Angle/ $^\circ$	Atom	Atom	Atom	Angle/ $^\circ$
O1	S01	C1	106.09(7)	N10	C11	O12	113.09(12)
O1	S01	C2	105.11(6)	N14	C11	O12	119.08(12)
C1	S01	C2	98.01(7)	N14	C11	N10	127.83(13)
C11	O12	C8	101.49(11)	N7	C8	O12	123.58(12)
C11	N10	N9	105.59(11)	N9	C8	O12	112.83(12)
N7 ¹	N7	C8	113.35(15)	N9	C8	N7	123.59(13)
C8	N9	N10	106.99(12)				

¹-X,1-Y,1-Z

Table S8 Torsion Angles for 4.

A	B	C	D	Angle/ $^\circ$	A	B	C	D	Angle/ $^\circ$
N10	N9	C8	O12	-0.99(16)	C11	O12	C8	N7	-179.08(13)
N10	N9	C8	N7	179.35(13)	C11	O12	C8	N9	1.26(15)
N7 ¹	N7	C8	O12	-0.2(2)	C11	N10	N9	C8	0.27(15)
N7 ¹	N7	C8	N9	179.39(15)	C8	O12	C11	N10	-1.08(15)
N9	N10	C11	O12	0.55(16)	C8	O12	C11	N14	178.79(13)
N9	N10	C11	N14	-179.30(14)					

¹-X,1-Y,1-Z

Table S9 Hydrogen Atom Coordinates ($\text{\AA} \times 10^4$) and Isotropic Displacement Parameters ($\text{\AA}^2 \times 10^3$) for 4.

Atom	x	y	z	U(eq)
H14A	8602.85	778.57	6250.61	19
H14B	7488.74	1152.01	4687.45	19
H1A	8790.9	3717.69	929.03	22
H1B	8233.54	3498.04	-743.25	22
H1C	10486.31	2270.16	115.16	22
H2A	3713.96	1688.02	2026.11	22
H2B	4085.21	3104.68	396.5	22
H2C	4938.13	3414.91	1961.32	22

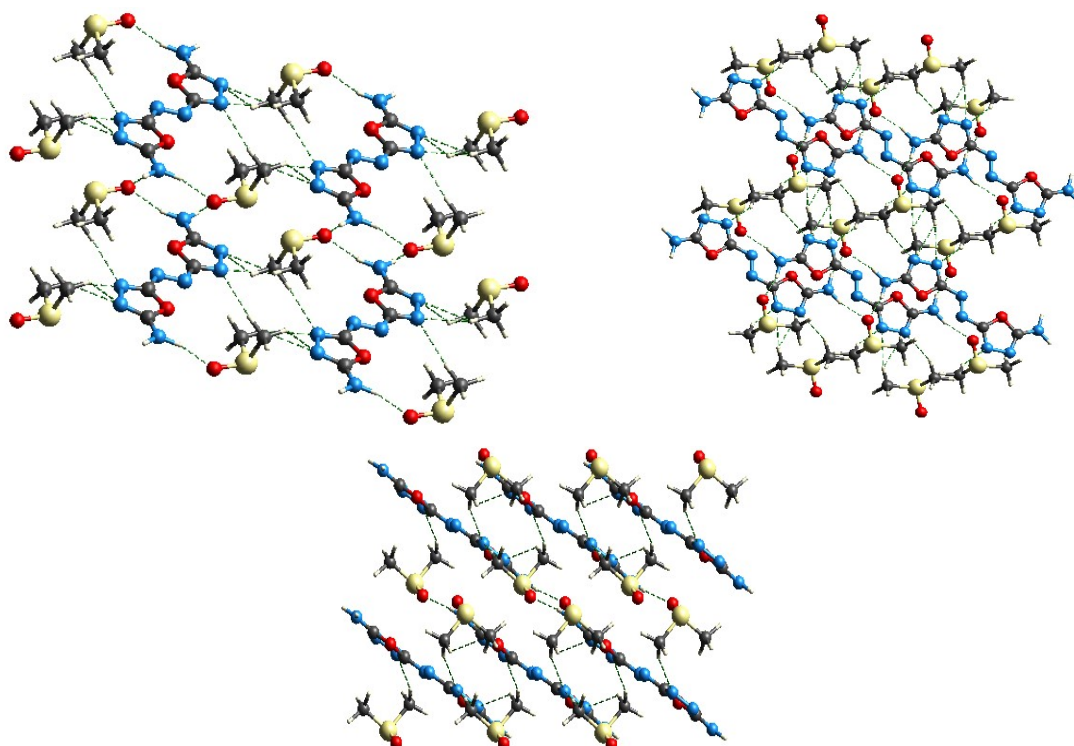


Figure S2: a) Packing diagram along the a-axis. b) Packing diagram along the b-axis. c) Packing diagram along the c-axis.

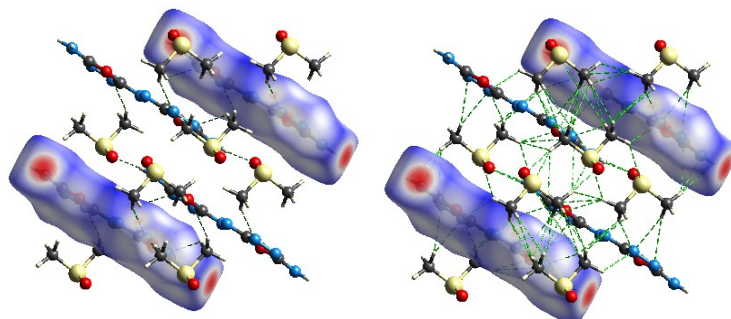


Figure S3: Hirshfeld surfaces of compound 4 showing H-bonding interactions and $\pi-\pi$ bond type interactions.

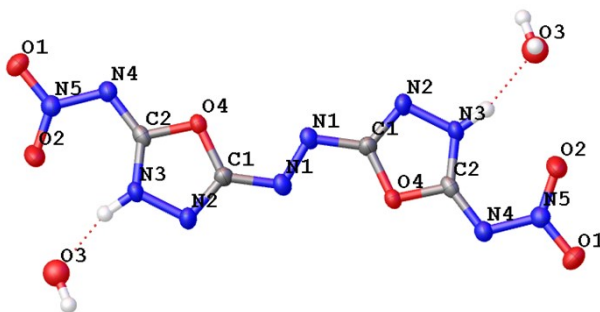


Figure S4: Molecular Structure of **5.** 2H₂O

Table S10 Crystal data and structure refinement for **5.** 2H₂O

CCDC No.	2173452
Empirical formula	C ₂ H ₃ N ₅ O ₄
Formula weight	161.09
Temperature/K	100
Crystal system	monoclinic
Space group	C2/c
a/Å	24.375(3)
b/Å	5.2668(6)
c/Å	9.2236(12)
α/°	90
β/°	103.392(4)
γ/°	90
Volume/Å ³	1151.9(3)
Z	8
ρ _{calc} g/cm ³	1.858
μ/mm ⁻¹	0.176
F(000)	656.0
Crystal size/mm ³	0.33 × 0.22 × 0.22
Radiation	MoKα ($\lambda = 0.71073$)
2Θ range for data collection/°	6.874 to 61.226
Index ranges	-33 ≤ h ≤ 32, -7 ≤ k ≤ 7, -13 ≤ l ≤ 13

Reflections collected	7404
Independent reflections	1616 [$R_{\text{int}} = 0.0710$, $R_{\text{sigma}} = 0.0666$]
Data/restraints/parameters	1616/0/102
Goodness-of-fit on F^2	1.087
Final R indexes [$I \geq 2\sigma(I)$]	$R_1 = 0.0779$, $wR_2 = 0.1437$
Final R indexes [all data]	$R_1 = 0.1138$, $wR_2 = 0.1565$
Largest diff. peak/hole / e Å ⁻³	0.62/-0.58

Table S11 Fractional Atomic Coordinates ($\times 10^4$) and Equivalent Isotropic Displacement Parameters (Å² $\times 10^3$) for 5. U_{eq} is defined as 1/3 of the trace of the orthogonalised U_{ij} tensor.

Atom	x	y	z	U(eq)
O3	6958.3(8)	1470(4)	6834(2)	14.4(4)
O1	5822.7(9)	-501(4)	9822(2)	21.1(5)
O2	5613.6(9)	2728(5)	8355(2)	25.3(6)
N3	6316.8(11)	4295(5)	6879(3)	14.5(5)
N1	7346.1(10)	3483(5)	4937(3)	15.2(5)
N2	6604.0(10)	5158(5)	5861(3)	16.9(5)
N4	6396.7(10)	373(5)	8363(3)	15.7(5)
N5	5922.5(10)	943(5)	8855(3)	16.5(5)
C	6976.1(12)	3423(6)	5868(3)	14.2(6)
C1	6515.8(12)	2055(6)	7429(3)	13.4(6)
O4	5298.4(10)	6681(5)	6340(2)	25.4(5)

Table S12 Anisotropic Displacement Parameters (Å² $\times 10^3$) for 5. The Anisotropic displacement factor exponent takes the form: $-2\pi^2[h^2a^*{}^2U_{11}+2hka^*b^*U_{12}+\dots]$.

Atom	U ₁₁	U ₂₂	U ₃₃	U ₂₃	U ₁₃	U ₁₂
O3	11.9(10)	15.3(11)	17.4(9)	1.3(8)	5.8(8)	2.5(8)
O1	24.2(12)	21.3(13)	19.8(10)	5.0(9)	9.2(9)	-0.3(9)
O2	19.2(11)	33.6(14)	25.4(11)	11.6(10)	9.7(9)	11.6(10)
N3	13.1(12)	14.6(13)	17.8(11)	0.3(9)	7.4(9)	2.4(10)
N1	11.7(12)	15.3(13)	19.5(11)	-0.5(10)	5.2(10)	-0.2(9)
N2	15.1(12)	16.8(13)	21.1(11)	2.0(10)	9.3(10)	1.1(10)
N4	15.3(12)	16.9(13)	16.0(10)	1.1(10)	5.8(9)	2.6(10)
N5	16.0(13)	18.2(14)	15.6(11)	0.5(9)	4.5(10)	1.5(10)
C	14.1(14)	12.0(14)	17.3(12)	0.9(11)	5.6(11)	0.0(11)
C1	10.9(13)	14.3(15)	14.6(12)	-4.4(10)	2.5(10)	1.2(10)

Table S13 Bond Lengths for 5.

Atom	Atom	Length/Å	Atom	Atom	Length/Å
------	------	----------	------	------	----------

Table S13 Bond Lengths for 5.

Atom	Atom	Length/Å	Atom	Atom	Length/Å
O3	C	1.368(3)	N1	N1 ¹	1.268(5)
O3	C1	1.354(3)	N1	C	1.382(3)
O1	N5	1.238(3)	N2	C	1.287(4)
O2	N5	1.226(3)	N4	N5	1.370(3)
N3	N2	1.372(3)	N4	C1	1.314(4)
N3	C1	1.331(4)			

¹3/2-X,1/2-Y,1-Z**Table S14 Bond Angles for 5.**

Atom	Atom	Atom	Angle/ [°]	Atom	Atom	Atom	Angle/ [°]
C1	O3	C	104.0(2)	O2	N5	N4	122.4(2)
C1	N3	N2	110.8(2)	O3	C	N1	123.1(2)
N1 ¹	N1	C	112.4(3)	N2	C	O3	114.1(2)
C	N2	N3	103.4(2)	N2	C	N1	122.8(3)
C1	N4	N5	113.6(2)	N3	C1	O3	107.5(2)
O1	N5	N4	115.2(2)	N4	C1	O3	115.5(3)
O2	N5	O1	122.4(2)	N4	C1	N3	137.0(3)

¹3/2-X,1/2-Y,1-Z**Table S15 Torsion Angles for 5.**

A	B	C	D	Angle/ [°]	A	B	C	D	Angle/ [°]
N3	N2	C	O3	-0.5(3)	C	O3	C1	N3	-3.2(3)
N3	N2	C	N1	177.1(3)	C	O3	C1	N4	177.2(2)
N1 ¹	N1	C	O3	1.3(5)	C1	O3	C	N1	-175.2(3)
N1 ¹	N1	C	N2	-176.1(3)	C1	O3	C	N2	2.3(3)
N2	N3	C1	O3	3.1(3)	C1	N3	N2	C	-1.6(3)
N2	N3	C1	N4	-177.4(3)	C1	N4	N5	O1	-174.8(2)
N5	N4	C1	O3	-175.5(2)	C1	N4	N5	O2	6.5(4)
N5	N4	C1	N3	5.1(5)					

¹3/2-X,1/2-Y,1-Z**Table S16 Hydrogen Atom Coordinates (Å×10⁴) and Isotropic Displacement Parameters (Å²×10³) for 5.**

Atom	x	y	z	U(eq)
H3	5998(17)	5050(80)	6920(40)	30(10)
H4A	5337.5	8105.43	5942.64	38
H4B	5074.63	5855.06	5659.53	38

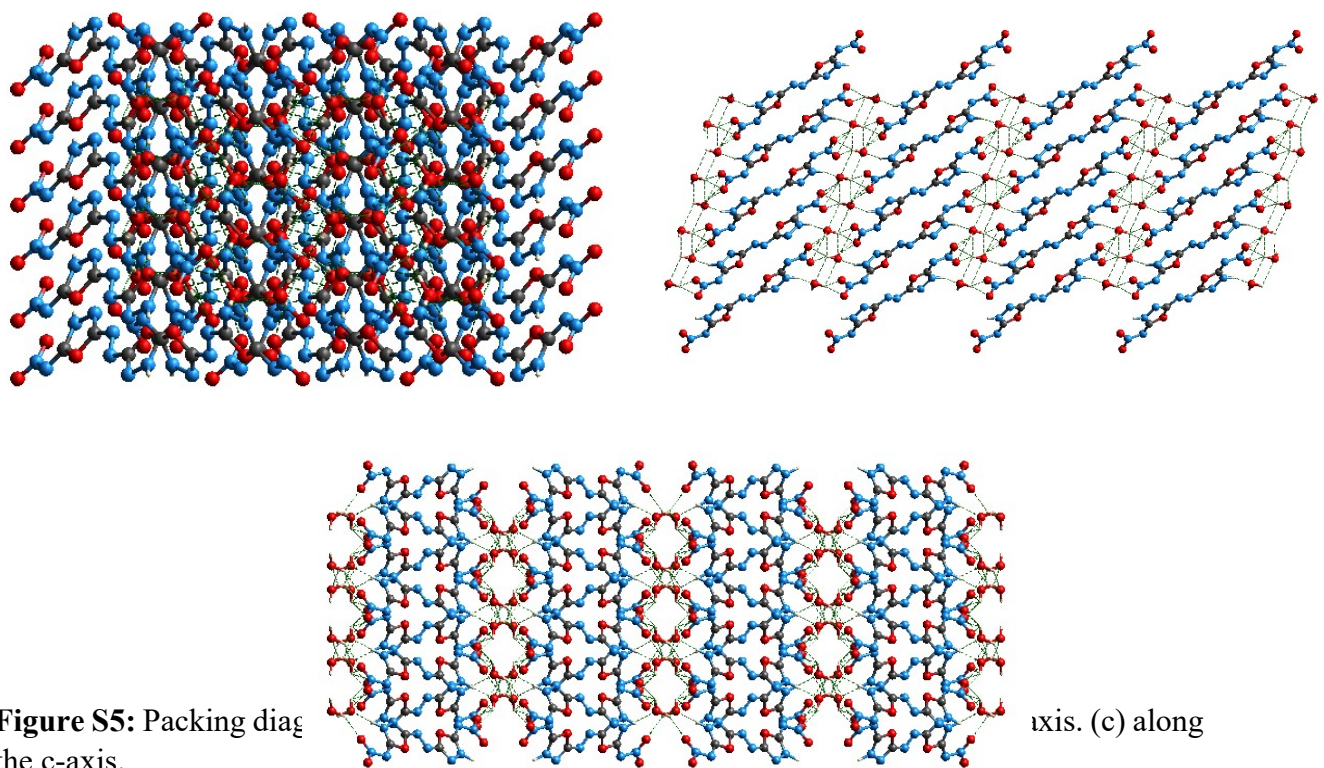


Figure S5: Packing diagrams along the c-axis.

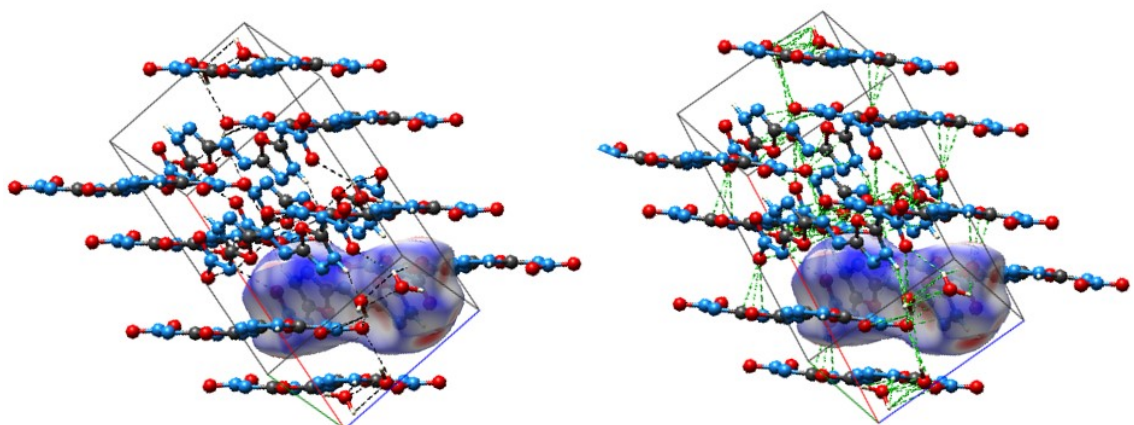


Figure S6: Hirshfeld surfaces of compound **5** showing H-bonding interactions and π - π bond type interactions in a unit cell.

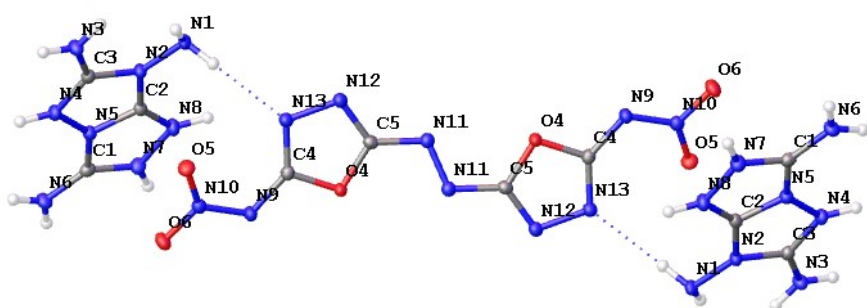


Figure S7: Molecular Structure of **7**.

Table S17 Crystal data and structure refinement for **7**.

CCDC No.

2173451

Empirical formula	C ₅ H ₈ N ₁₃ O ₃
Formula weight	298.24
Temperature/K	100
Crystal system	Triclinic
Space group	P-1
a/Å	6.7799(6)
b/Å	6.8854(6)
c/Å	12.8125(12)
$\alpha/^\circ$	77.172(3)
$\beta/^\circ$	89.270(3)
$\gamma/^\circ$	69.344(2)
Volume/Å ³	544.29(9)
Z	2
$\rho_{\text{calc}} \text{g/cm}^3$	1.820
μ/mm^{-1}	0.152
F(000)	306.0
Crystal size/mm ³	0.33 × 0.22 × 0.22
Radiation	MoKα ($\lambda = 0.71073$)
2Θ range for data collection/°	6.438 to 56.712
Index ranges	-9 ≤ h ≤ 9, -9 ≤ k ≤ 9, -17 ≤ l ≤ 17
Reflections collected	8556
Independent reflections	2708 [R _{int} = 0.0382, R _{sigma} = 0.0400]
Data/restraints/parameters	2708/0/198
Goodness-of-fit on F ²	1.059
Final R indexes [I>=2σ (I)]	R ₁ = 0.0474, wR ₂ = 0.1271
Final R indexes [all data]	R ₁ = 0.0574, wR ₂ = 0.1365
Largest diff. peak/hole / e Å ⁻³	0.45/-0.71

Table S18 Fractional Atomic Coordinates ($\times 10^4$) and Equivalent Isotropic Displacement Parameters ($\text{\AA}^2 \times 10^3$) for 7. U_{eq} is defined as 1/3 of the trace of the orthogonalised U_{IJ} tensor.

Atom	x	y	z	$U(\text{eq})$
O4	7609.2(19)	4516.6(19)	1365.2(9)	14.0(3)
O5	1888(2)	5018(2)	2300.7(10)	18.5(3)
O6	3367(2)	3399(2)	3911.2(10)	19.3(3)
N11	9178(2)	5826(2)	-188.9(11)	13.9(3)
N2	-437(2)	9440(2)	2293.3(11)	13.9(3)
N9	5424(2)	4035(2)	2641.6(12)	14.8(3)
N5	-56(2)	8208(2)	4011.4(11)	13.5(3)
N13	4270(2)	6684(2)	896.2(11)	14.4(3)
N4	-2109(2)	8372(2)	3742.3(12)	14.6(3)
N10	3489(2)	4189(2)	2932.6(12)	14.6(3)
N12	5533(2)	7199(2)	101.9(11)	14.5(3)
N8	2876(2)	8702(3)	3411.4(12)	17.0(3)
N6	834(2)	6995(2)	5902.6(12)	17.0(3)
N7	3019(2)	7941(2)	4531.9(12)	17.4(3)
N1	-82(2)	9858(3)	1200.7(11)	15.5(3)
N3	-3855(2)	9364(2)	2019.2(12)	17.0(3)
C5	7457(3)	5895(3)	399.8(13)	13.8(3)
C2	959(3)	8835(3)	3164.7(13)	14.0(3)
C4	5562(3)	5108(3)	1639.2(14)	13.4(3)
C3	-2224(3)	9071(3)	2684.7(14)	13.6(3)
C1	1256(3)	7639(3)	4898.0(14)	14.5(3)

Table S19 Anisotropic Displacement Parameters ($\text{\AA}^2 \times 10^3$) for 7. The Anisotropic displacement factor exponent takes the form: $-2\pi^2[h^2a^*{}^2U_{11}+2hka^*b^*U_{12}+\dots]$.

Atom	U_{11}	U_{22}	U_{33}	U_{23}	U_{13}	U_{12}
------	----------	----------	----------	----------	----------	----------

Table S19 Anisotropic Displacement Parameters ($\text{\AA}^2 \times 10^3$) for **7**. The Anisotropic displacement factor exponent takes the form: $-2\pi^2[h^2a^*{}^2U_{11} + 2hka^*b^*U_{12} + \dots]$.

Atom	U ₁₁	U ₂₂	U ₃₃	U ₂₃	U ₁₃	U ₁₂
O4	12.5(6)	15.5(6)	11.4(6)	-0.6(4)	1.9(4)	-3.6(5)
O5	14.4(6)	22.9(7)	16.3(6)	-2.1(5)	-2.5(5)	-5.7(5)
O6	19.2(7)	26.1(7)	12.4(6)	-0.5(5)	1.7(5)	-10.3(5)
N11	13.7(7)	15.2(7)	12.9(7)	-3.6(5)	0.9(5)	-5.0(6)
N2	11.3(7)	17.9(7)	11.4(7)	-1.8(5)	1.0(5)	-4.8(5)
N9	12.4(7)	18.1(7)	12.8(7)	-1.1(5)	1.5(5)	-5.5(6)
N5	12.4(7)	15.7(7)	12.3(7)	-2.5(5)	0.6(5)	-5.2(5)
N13	14.4(7)	15.6(7)	11.7(7)	-1.7(5)	1.0(5)	-4.5(6)
N4	10.9(7)	18.7(7)	14.7(7)	-2.8(6)	1.6(5)	-6.7(6)
N10	14.5(7)	14.9(7)	14.0(7)	-3.2(5)	1.1(5)	-4.8(5)
N12	15.0(7)	15.6(7)	12.4(7)	-2.8(5)	1.5(5)	-5.2(6)
N8	13.5(7)	23.2(8)	14.6(7)	-4.5(6)	1.1(5)	-6.9(6)
N6	17.1(7)	21.6(7)	11.4(7)	-1.0(6)	-1.1(6)	-7.3(6)
N7	14.7(7)	22.5(8)	14.3(7)	-3.7(6)	-0.6(6)	-6.2(6)
N1	15.9(7)	17.5(7)	10.7(7)	-1.0(6)	4.0(5)	-4.5(6)
N3	14.1(7)	23.0(8)	13.2(7)	-0.2(6)	-1.3(5)	-8.2(6)
C5	15.7(8)	13.4(7)	11.9(7)	-2.6(6)	-0.1(6)	-5.1(6)
C2	14.1(8)	14.4(8)	12.8(8)	-2.7(6)	2.6(6)	-4.7(6)
C4	12.4(8)	14.5(8)	13.9(8)	-4.2(6)	1.1(6)	-5.1(6)
C3	12.8(8)	13.6(7)	14.5(8)	-3.7(6)	1.8(6)	-4.6(6)
C1	14.2(8)	13.4(8)	14.7(8)	-4.1(6)	-0.4(6)	-3.1(6)

Table S20 Bond Lengths for **7**.

Atom	Atom	Length/ \AA	Atom	Atom	Length/ \AA
O4	C5	1.362(2)	N5	C2	1.349(2)

Table S20 Bond Lengths for 7.

Atom	Atom	Length/Å	Atom	Atom	Length/Å
O4	C4	1.367(2)	N5	C1	1.348(2)
O5	N10	1.2406(19)	N13	N12	1.388(2)
O6	N10	1.2655(19)	N13	C4	1.320(2)
N11	N11 ¹	1.283(3)	N4	C3	1.327(2)
N11	C5	1.374(2)	N12	C5	1.299(2)
N2	N1	1.4007(19)	N8	N7	1.407(2)
N2	C2	1.363(2)	N8	C2	1.307(2)
N2	C3	1.389(2)	N6 C1	1.327(2)	
N9	N10	1.334(2)	N7 C1	1.345(2)	
N9	C4	1.352(2)	N3 C3	1.334(2)	
N5	N4	1.398(2)			

¹2-X,1-Y,-Z**Table S21** Bond Angles for 7.

Atom	Atom	Atom	Angle/°	Atom	Atom	Atom	Angle/°
C5	O4	C4	102.43(13)	C1	N7	N8	112.95(14)
N11 ¹	N11	C5	112.84(18)	O4	C5	N11	122.21(15)
C2	N2	N1	129.20(14)	N12	C5	O4	112.73(15)
C2	N2	C3	105.59(14)	N12	C5	N11	125.03(15)
C3	N2	N1	123.62(14)	N5	C2	N2	105.53(15)
N10	N9	C4	116.63(14)	N8	C2	N2	140.22(16)
C2	N5	N4	113.90(14)	N8	C2	N5	114.24(15)
C1	N5	N4	138.52(15)	N9	C4	O4	111.03(14)
C1	N5	C2	107.56(15)	N13	C4	O4	112.07(15)
C4	N13	N12	105.92(14)	N13	C4	N9	136.64(16)
C3	N4	N5	100.72(13)	N4	C3	N2	114.18(15)
O5	N10	O6	120.80(14)	N4	C3	N3	124.95(16)
O5	N10	N9	123.56(14)	N3	C3	N2	120.84(15)

Table S21 Bond Angles for 7.

Atom	Atom	Atom	Angle/ $^{\circ}$	Atom	Atom	Atom	Angle/ $^{\circ}$
O6	N10	N9	115.64(14)	N6	C1	N5	126.69(16)
C5	N12	N13	106.83(14)	N6	C1	N7	128.79(16)
C2	N8	N7	100.75(14)	N7	C1	N5	104.49(15)

¹²-X,¹-Y,-Z**Table S22** Torsion Angles for 7.

A	B	C	D	Angle/ $^{\circ}$	A	B	C	D	Angle/ $^{\circ}$
N11 ¹	N11	C5	O4	9.4(3)	N1	N2	C3	N4	169.70(15)
N11 ¹	N11	C5	N12	-168.65(18)	N1	N2	C3	N3	-8.7(3)
N5	N4	C3	N2	-2.81(18)	C5	O4	C4	N9	-173.98(14)
N5	N4	C3	N3	175.46(16)	C5	O4	C4	N13	1.05(18)
N13	N12	C5	O4	-0.83(19)	C2	N2	C3	N4	2.9(2)
N13	N12	C5	N11	177.35(16)	C2	N2	C3	N3	-175.42(16)
N4	N5	C2	N2	-0.10(19)	C2	N5	N4	C3	1.76(18)
N4	N5	C2	N8	179.51(14)	C2	N5	C1	N6	177.56(16)
N4	N5	C1	N6	-0.4(3)	C2	N5	C1	N7	-0.49(18)
N4	N5	C1	N7	-178.50(18)	C2	N8	N7	C1	0.59(19)
N10	N9	C4	O4	-168.67(14)	C4	O4	C5	N11	-178.32(15)
N10	N9	C4	N13	18.0(3)	C4	O4	C5	N12	-0.09(18)
N12	N13	C4	O4	-1.55(19)	C4	N9	N10	O5	9.4(2)
N12	N13	C4	N9	171.7(2)	C4	N9	N10	O6	-171.59(15)
N8	N7	C1	N5	-0.06(19)	C4	N13	N12	C5	1.42(18)
N8	N7	C1	N6	-178.06(16)	C3	N2	C2	N5	-1.56(18)
N7	N8	C2	N2	178.5(2)	C3	N2	C2	N8	179.0(2)
N7	N8	C2	N5	-0.92(19)	C1	N5	N4	C3	179.7(2)
N1	N2	C2	N5	-167.32(16)	C1	N5	C2	N2	-178.66(14)
N1	N2	C2	N8	13.2(4)	C1	N5	C2	N8	1.0(2)

¹²-X,¹-Y,-Z

Table S23 Hydrogen Atom Coordinates ($\text{\AA} \times 10^4$) and Isotropic Displacement Parameters ($\text{\AA}^2 \times 10^3$) for 7.

Atom	x	y	z	U(ϵ)
H4	-3061.69	8089.26	4159.19	18
H6A	1781.52	6704.3	6433.2	20
H6B	-392.07	6859.46	6038.18	20
H7	4144.49	7688.11	4949.61	21
H3A	-4962.29	9088.52	2275.16	20
H3B	-3822.26	9833.95	1324.34	20
H1A	200(40)	11070(40)	1042(19)	25(6)
H1B	1070(40)	8800(40)	1101(17)	15(5)

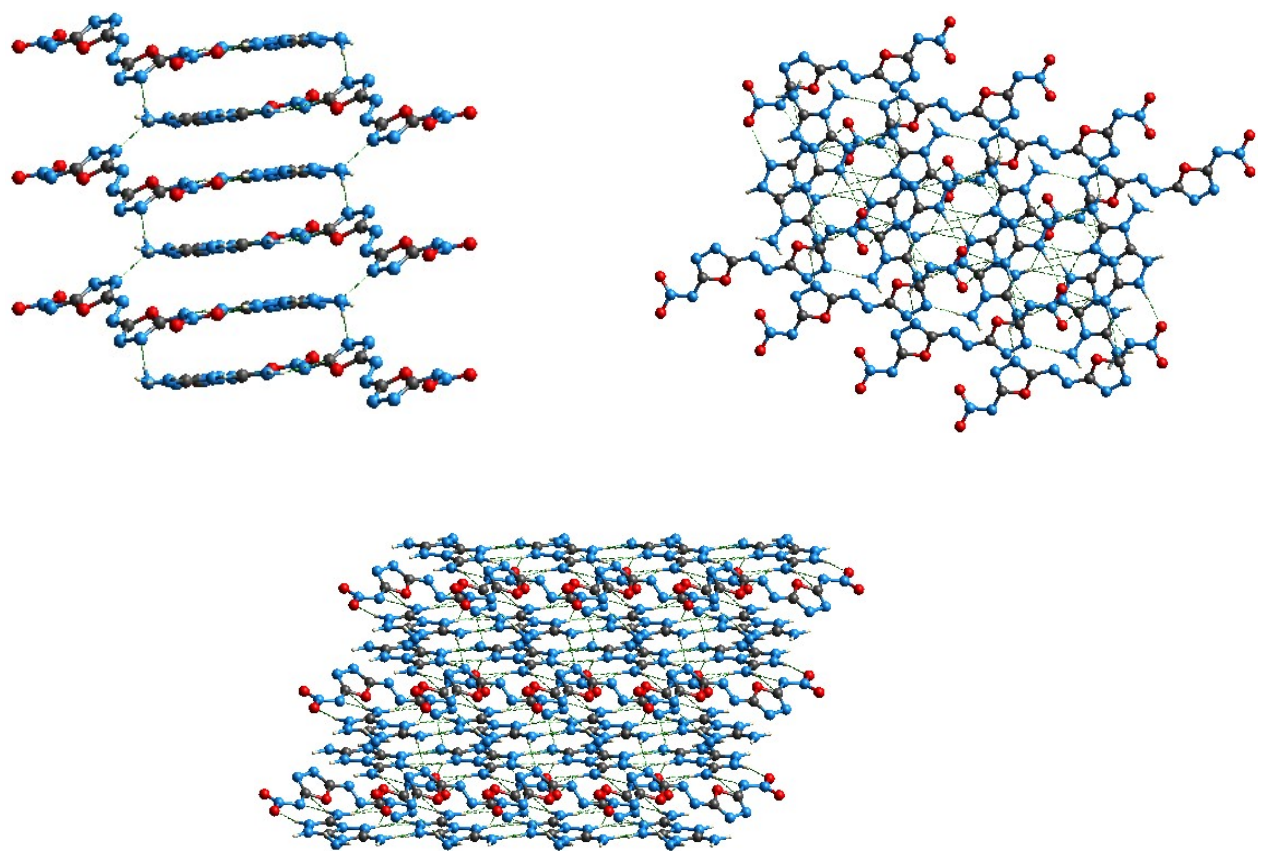


Figure S8: Packing diagram of compound 7, (a) along the **a**-axis, (b) along the **b**-axis, (c) along the **c**-axis.

Resazurin-based cell viability assay.

HEK-293 cells (p# 37) were cultured in D1 complete media (DMEM supplemented with 10% FBS and 1% Penicillin-Streptomycin antibiotic solution) at 37 °C in a 5% CO₂ atmosphere. Then the cells were trypsinized, counted, and plated in 96-well clear, flat-bottom microplates (NEST), at a density of 2.5×10^3 cells per well in 150 µl DMEM complete medium and incubated for 24 hours at 37 °C in a 5% CO₂ incubator. After 24 h of incubation, cells were treated in triplicate with indicated test compounds at 50 µM, 25 µM, 12.5 µM and 6.25 µM concentrations, 0.05% DMSO (negative control) and 533 nM Doxorubicin (positive control) for 72 h in a CO₂ incubator. Cell viability was assessed after drug treatment using resazurin assay. Briefly, 1mg/mL solution of resazurin sodium (SRL) was prepared in 1X sterile PBS. Media from the wells with compounds was removed, wells were washed with 1X PBS once and a fresh DMEM media 100 µL/well was added. Then, 600 µL of 1mg/mL solution of resazurin was diluted with 9.4 mL DMEM culture media and 50 µL was added to all wells making the final concentration of 0.02 mg/mL resazurin sodium per well. Plates were incubated at 37 Degree Celsius in 5% CO₂ incubator for 4 hours in dark. After incubation, the fluorescence intensity was measured using GloMax® Explorer (Promega) instrument with 520 nm excitation and 580-640 nm emission filter. Percentage cell viability was calculated as ((fluorescence of treated cells- fluorescence of media control)/fluorescence of DMSO treated cells- fluorescence of media control)*100. Graphs were plotted using Graphpad Prism 8 software.

NMR, IR, Mass Spectra, and DSC plots

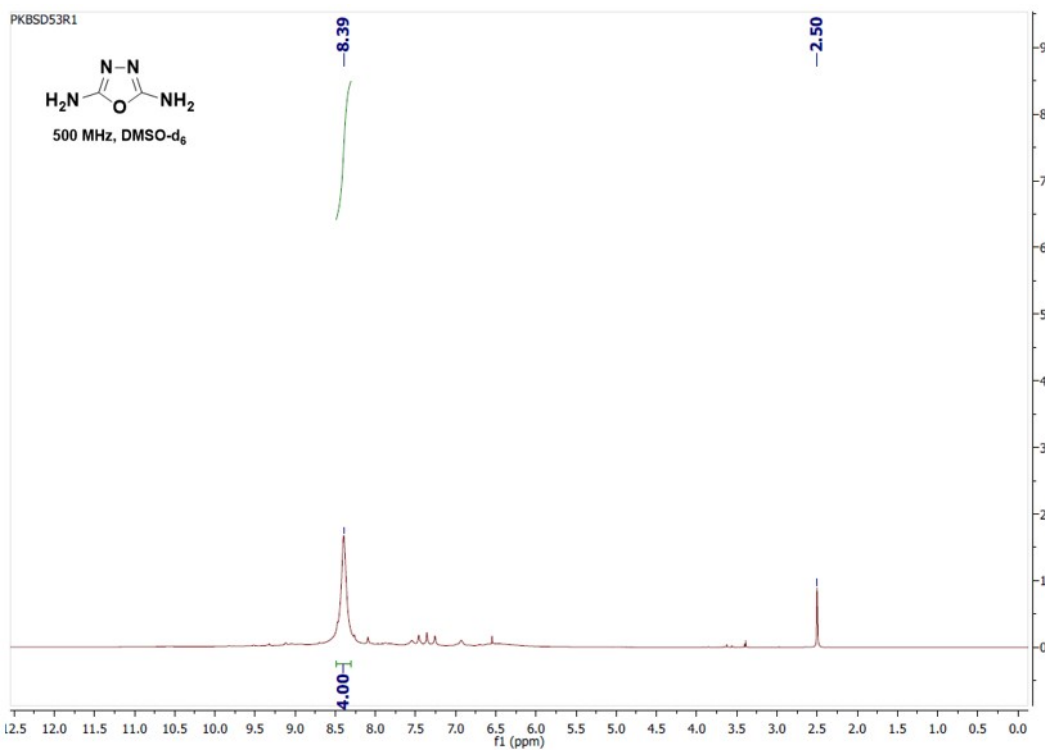


Fig.S9: ^1H NMR Spectra of 1,3,4-oxadiazole-2,5-diamine (1)

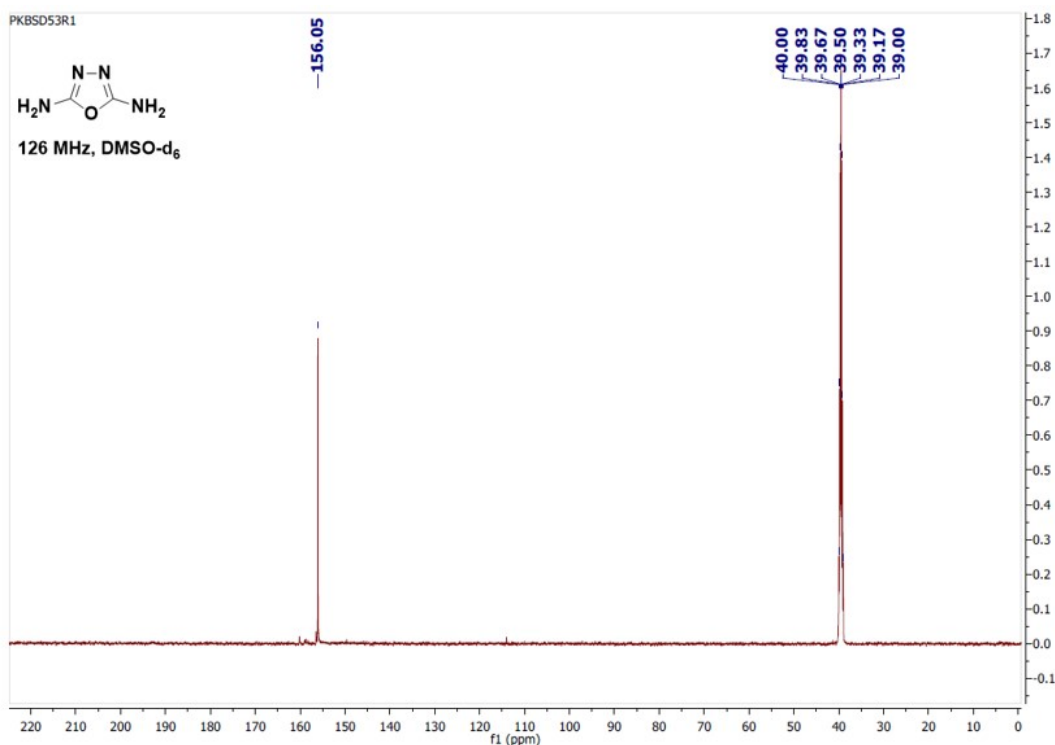


Fig.S10: ^{13}C NMR Spectra of 1,3,4-oxadiazole-2,5-diamine (1)

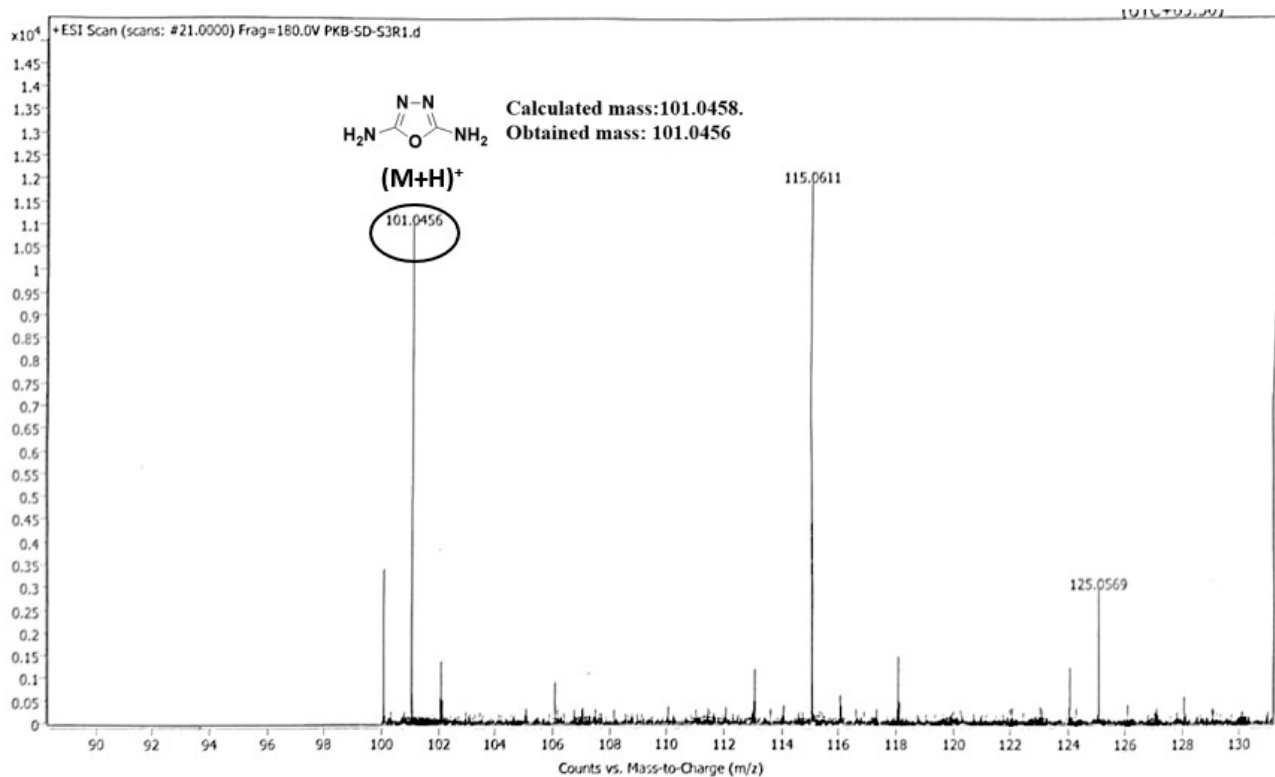


Fig.S11: Mass Spectra of Compound 1

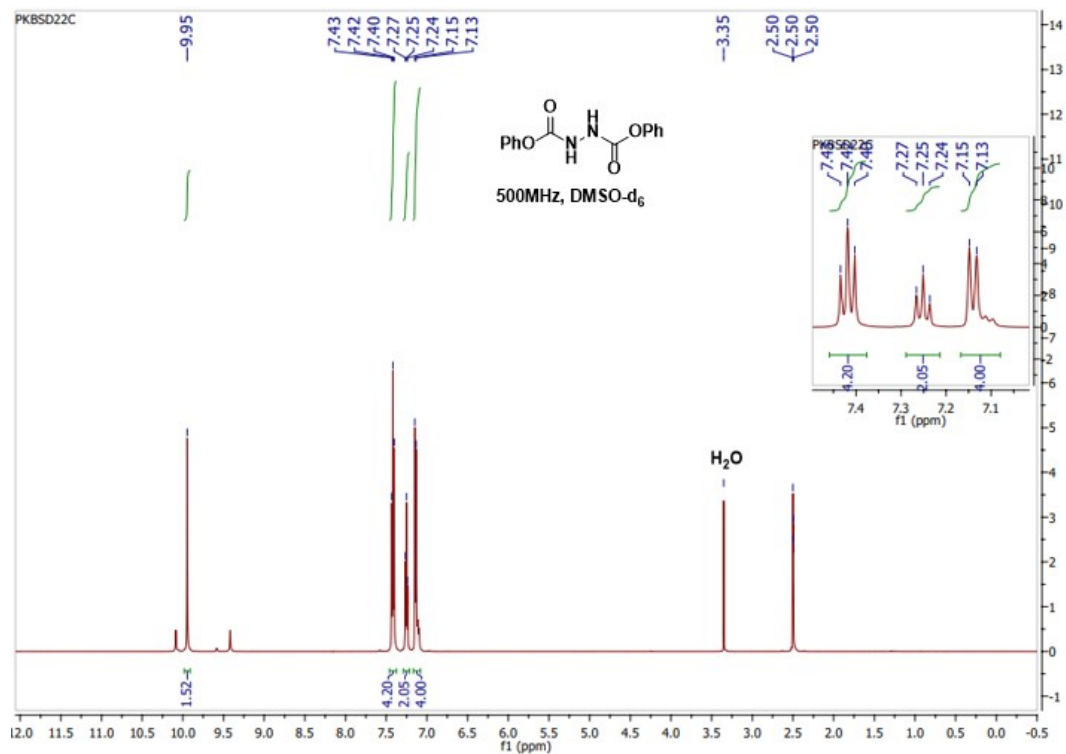


Fig.S12: ¹H NMR Spectra of Diphenyl hydrazodicarboxylate (diphenyl bicarbamate) (3b)

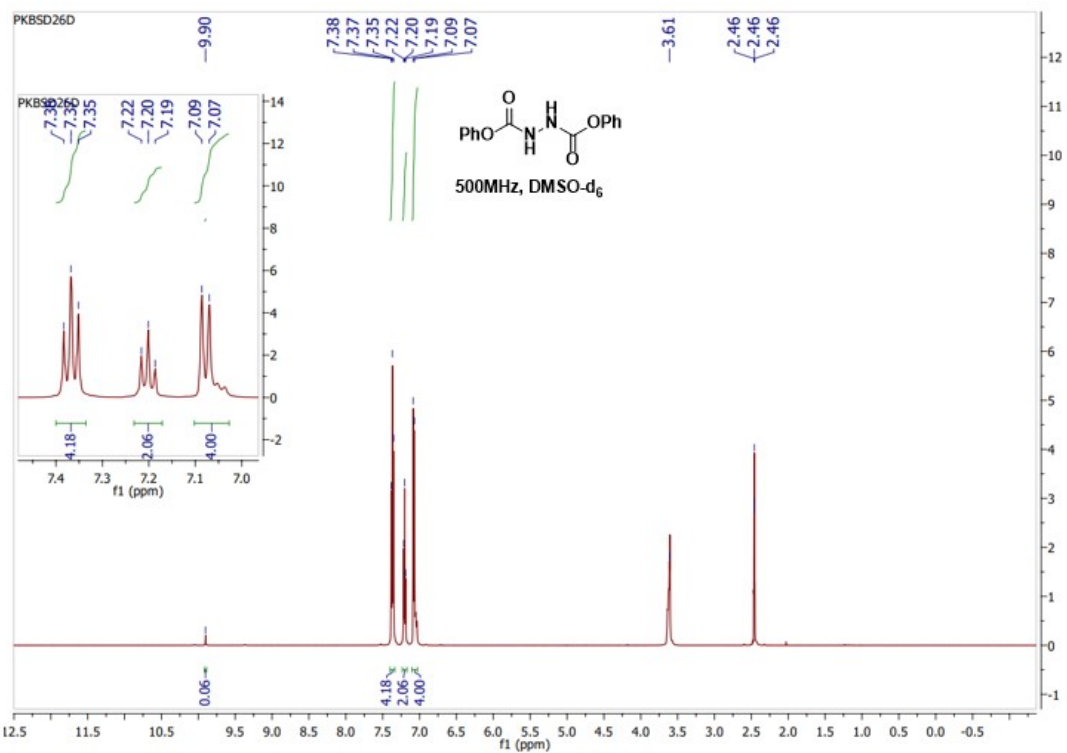


Fig.S13: ^1H NMR Spectra of Diphenyl hydrazodicarboxylate (diphenyl bicarbamate) (**3b**) with D_2O

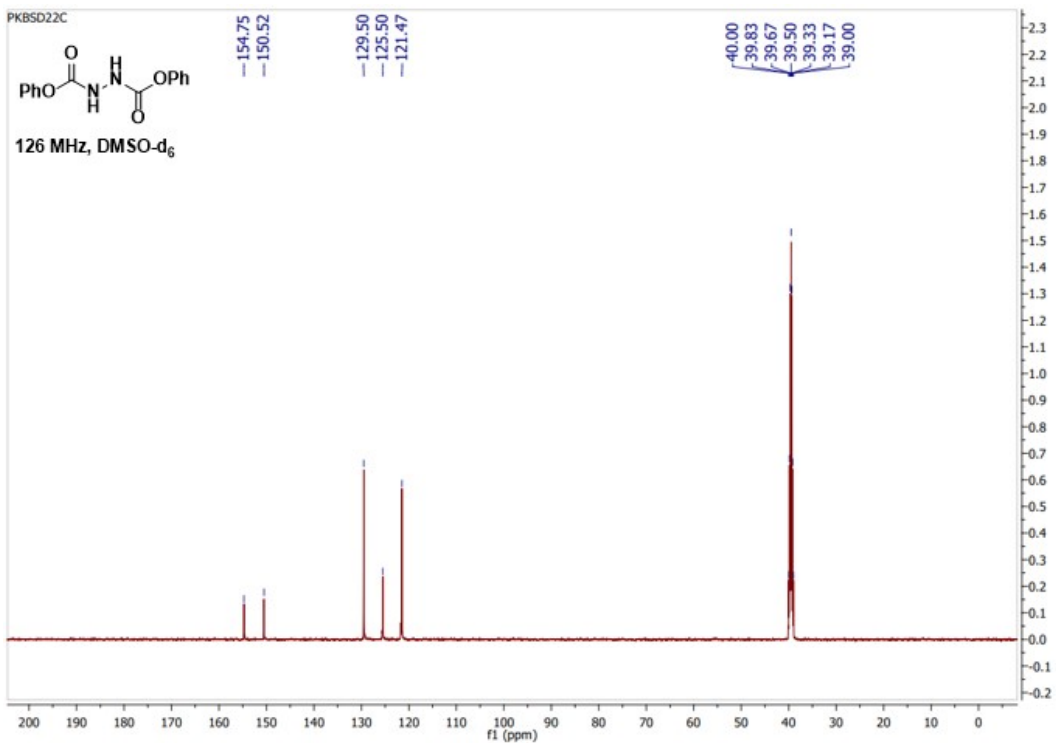


Fig.S14: ^{13}C NMR Spectra of Diphenyl hydrazodicarboxylate (diphenyl bicarbamate) (**3b**).

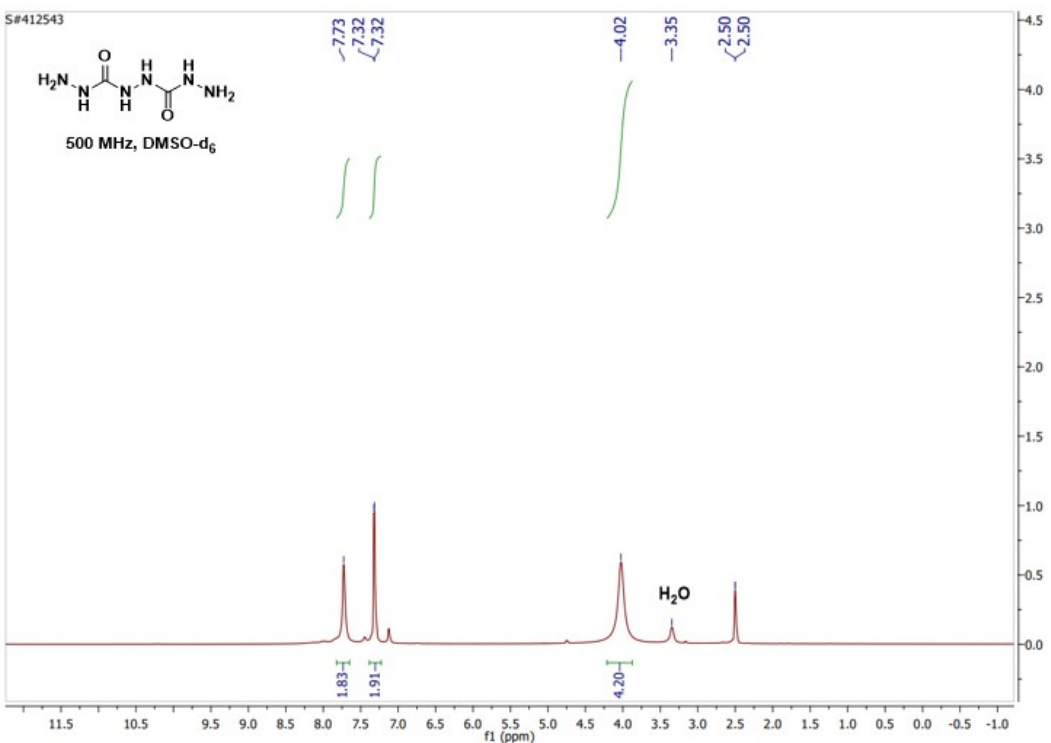


Fig.S15: ¹H NMR Spectra of Compound 3

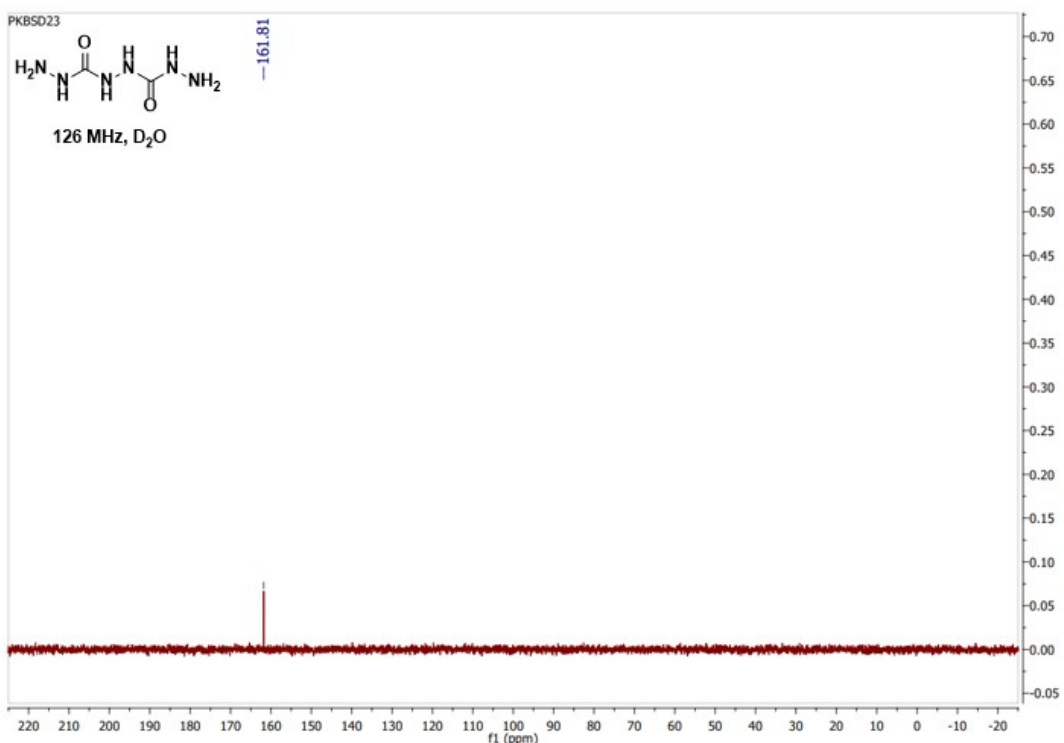


Fig.S16: ¹³C NMR Spectra of Compound 3

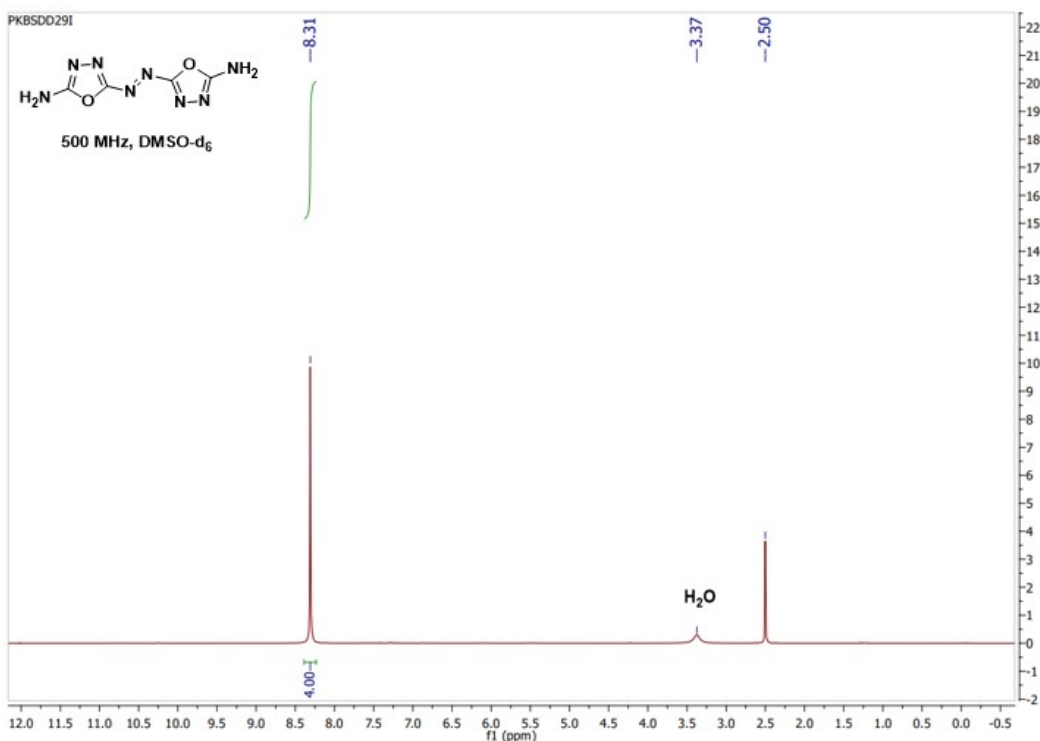


Fig.S17: ¹H NMR Spectra of Compound 4

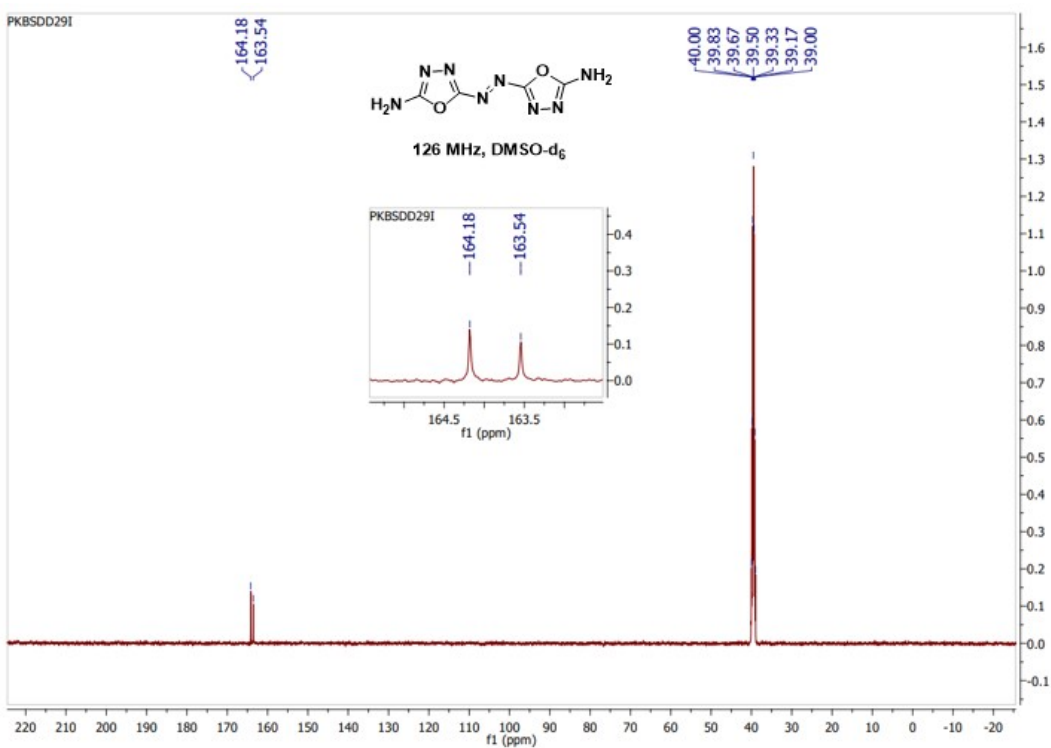


Fig.S18: ¹³C NMR Spectra of Compound 4

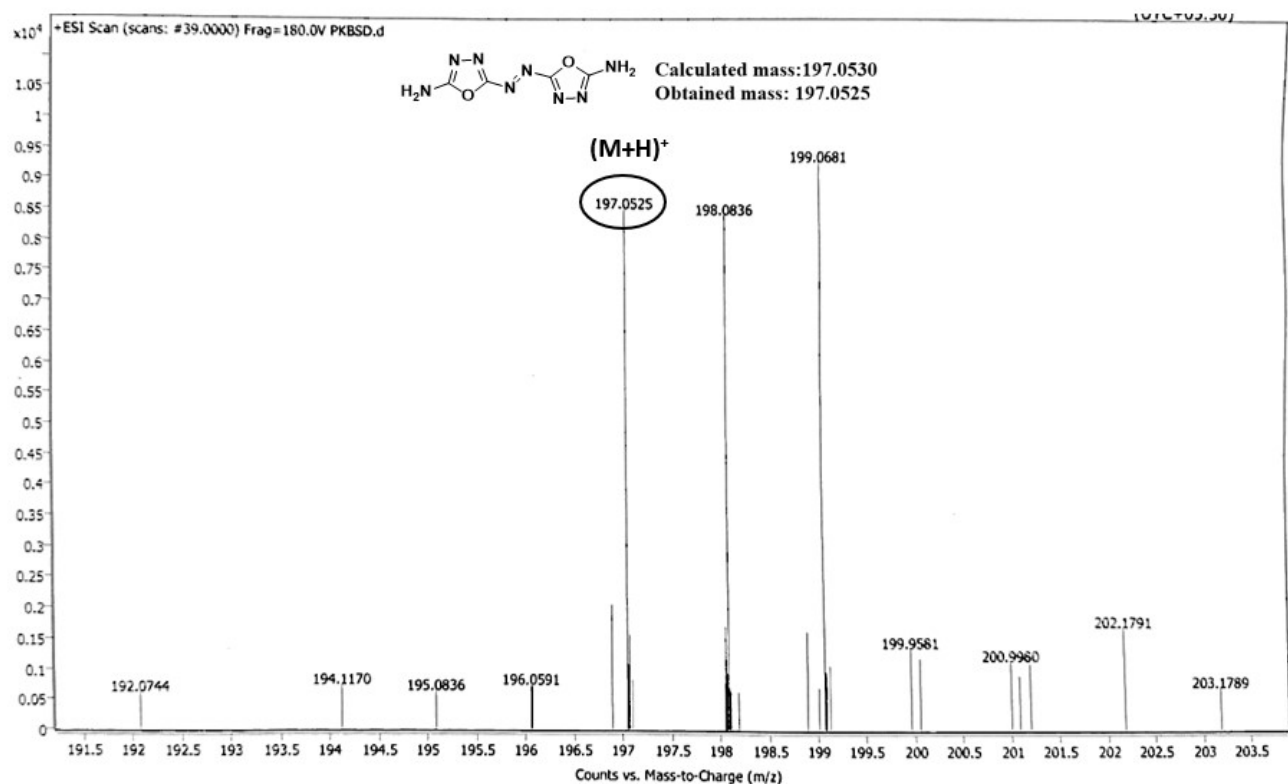


Fig.S19: Mass Spectra of Compound 4

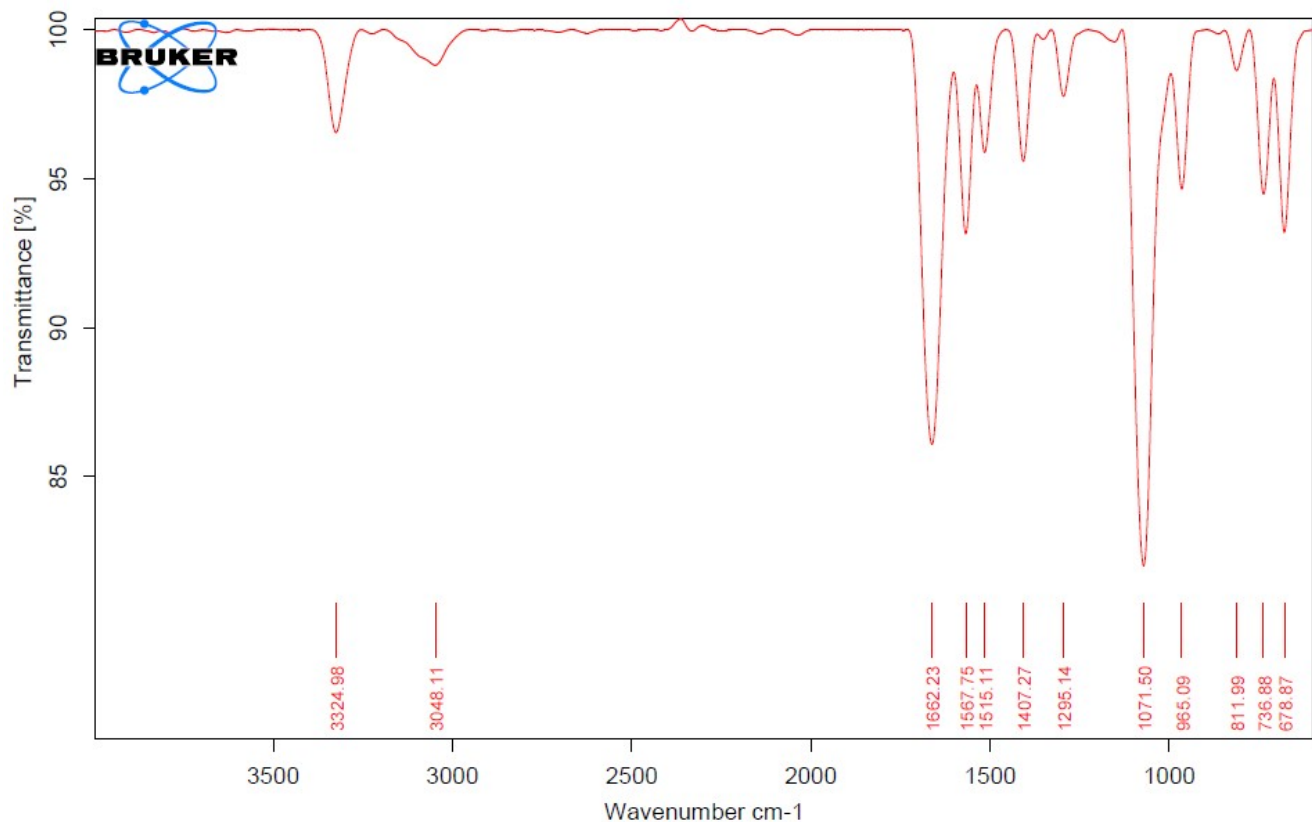
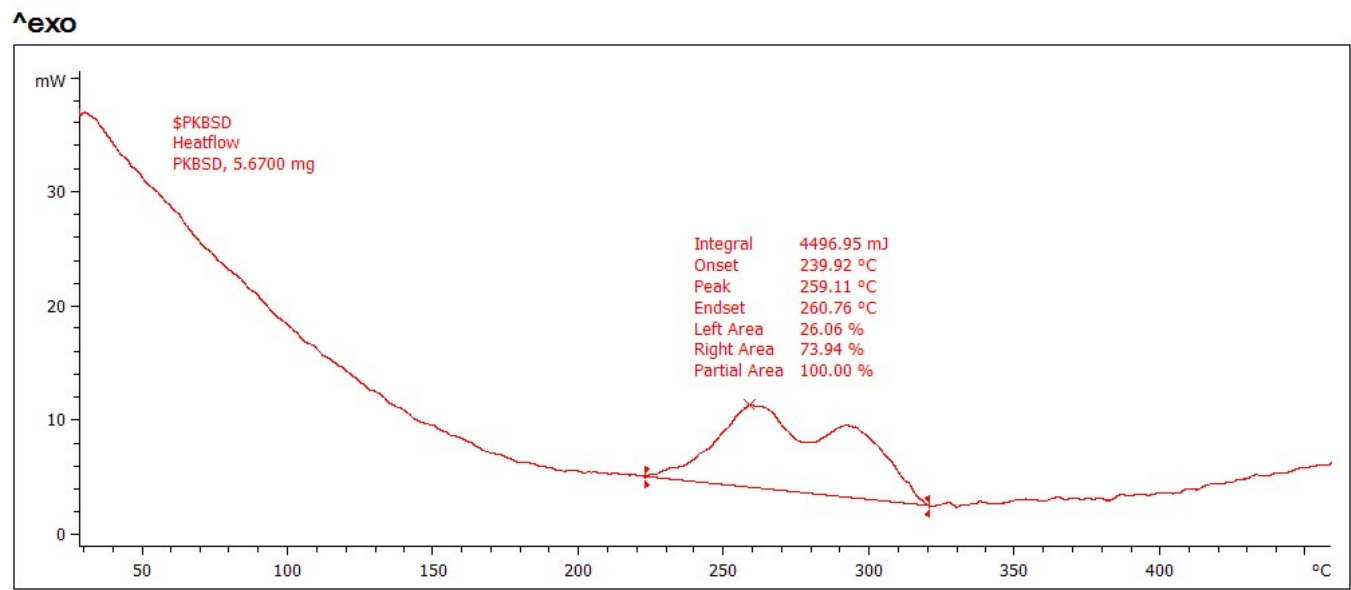


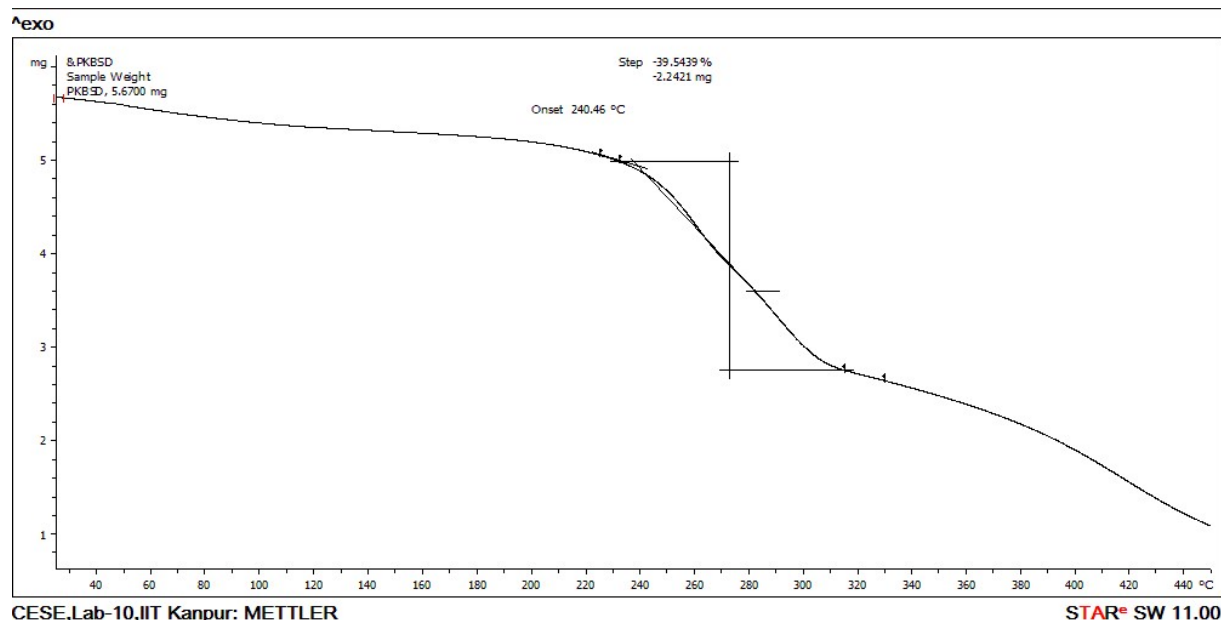
Fig.S20: IR Spectrum of Compound 4.



CESE,Lab-10,IIT Kanpur: METTLER

STAR^e SW 11.00

Fig S21. DSC Plot of Compound 4 at the Heating rate 5 °C min⁻¹.



CESE,Lab-10,IIT Kanpur: METTLER

STAR^e SW 11.00

Fig S22. TGA curve of Compound 4 at the Heating rate 5 °C min⁻¹.

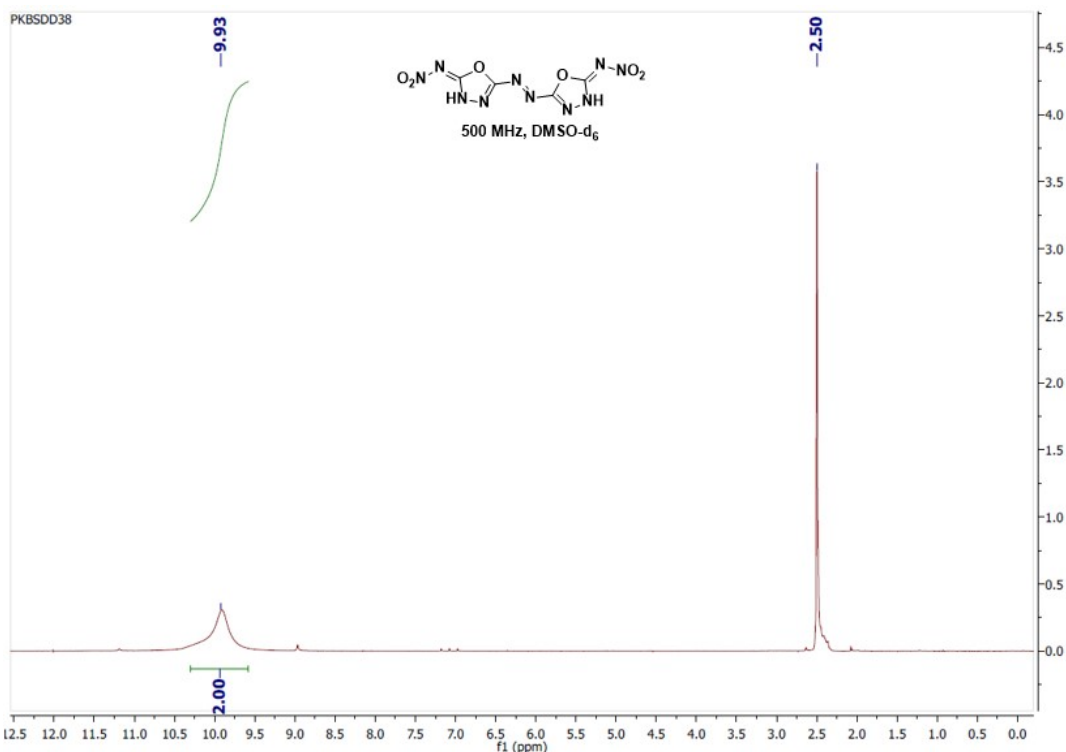


Fig.S23: ^1H NMR Spectra of Compound 5.

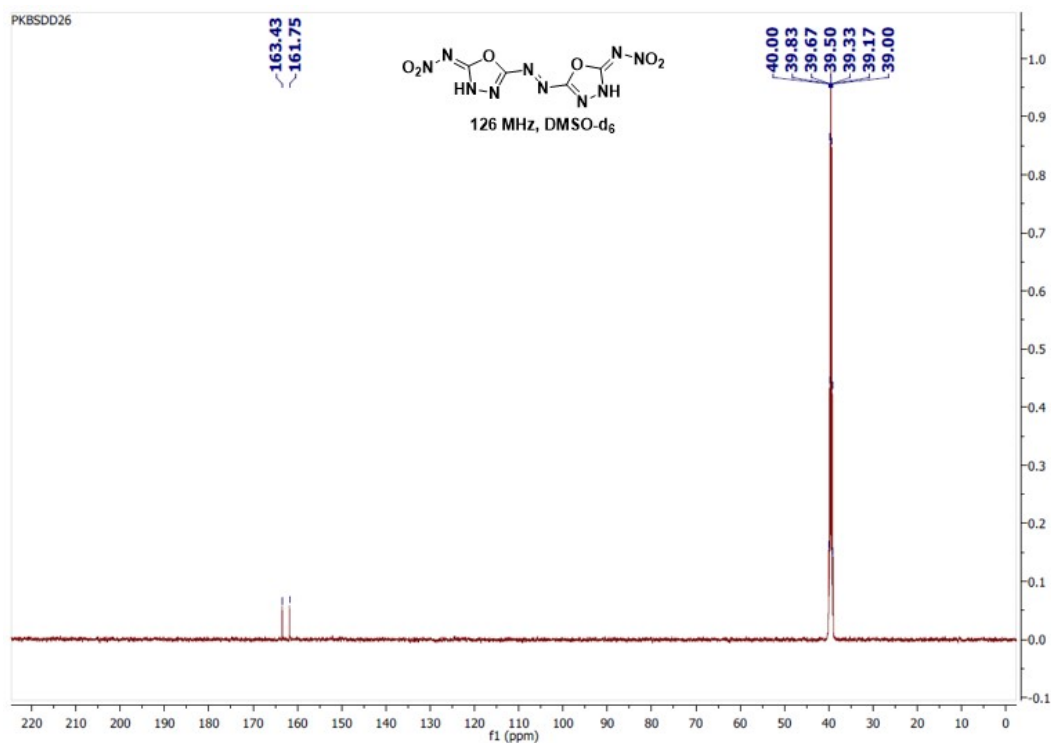


Fig.S24: ^{13}C NMR Spectra of Compound 5.

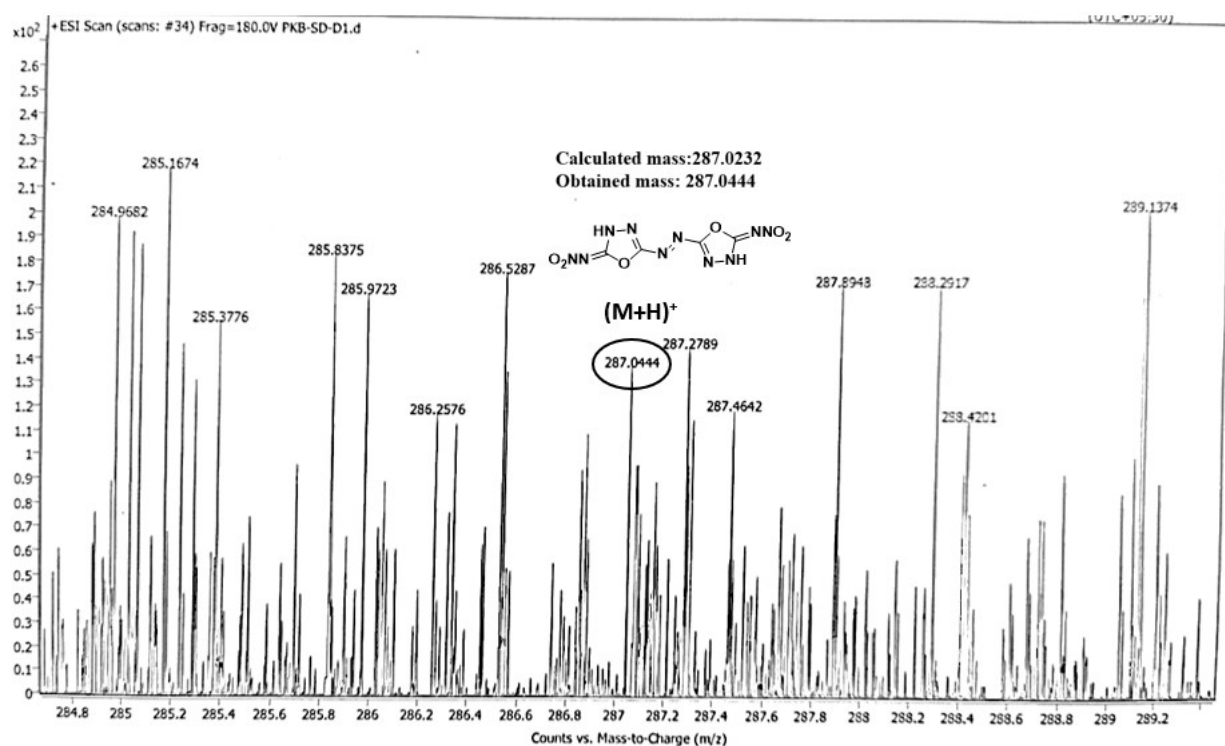


Fig.S25: Mass Spectra of Compound 5.

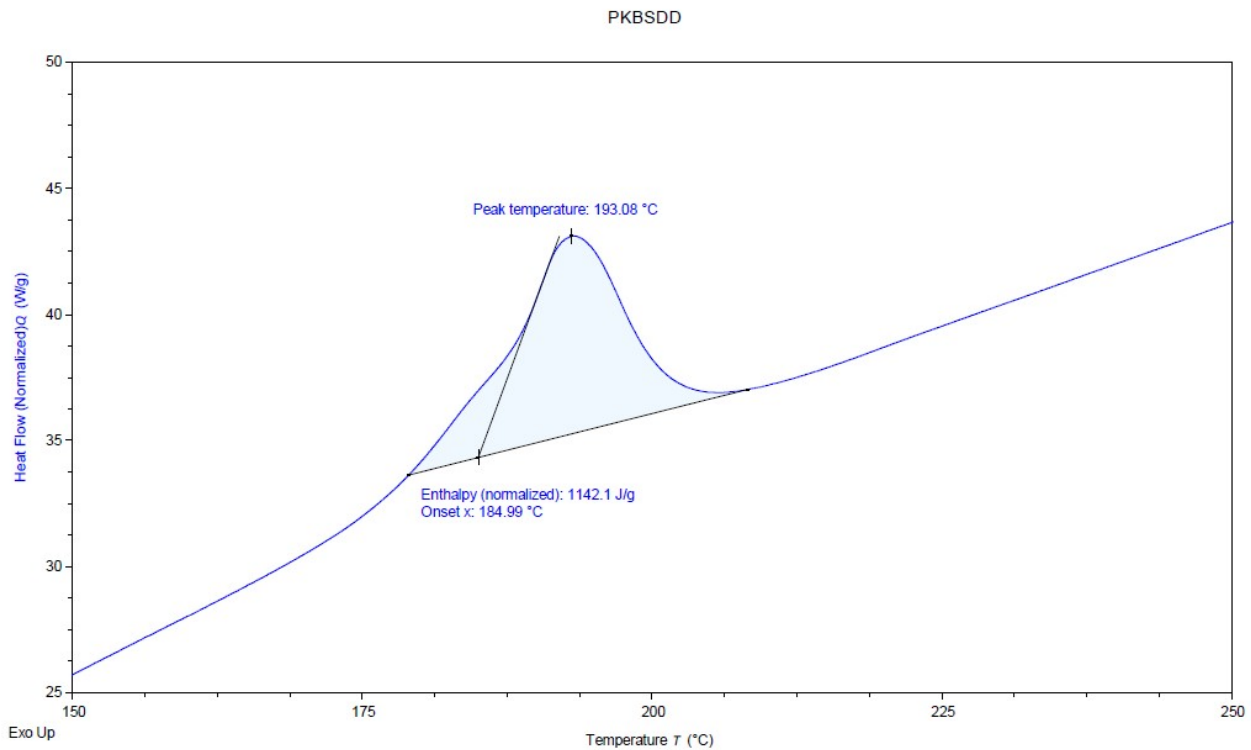


Fig S26. DSC Plot of Compound 5 at the Heating rate 5 °C min⁻¹.

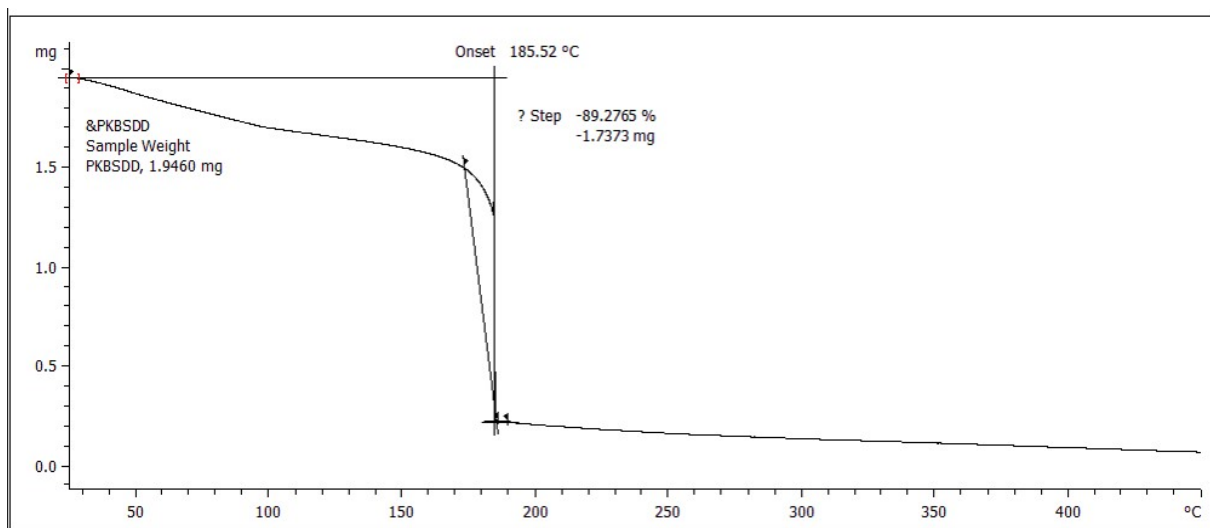


Fig S27. TGA Curve of Compound 5 at the Heating rate 5 °C min⁻¹.

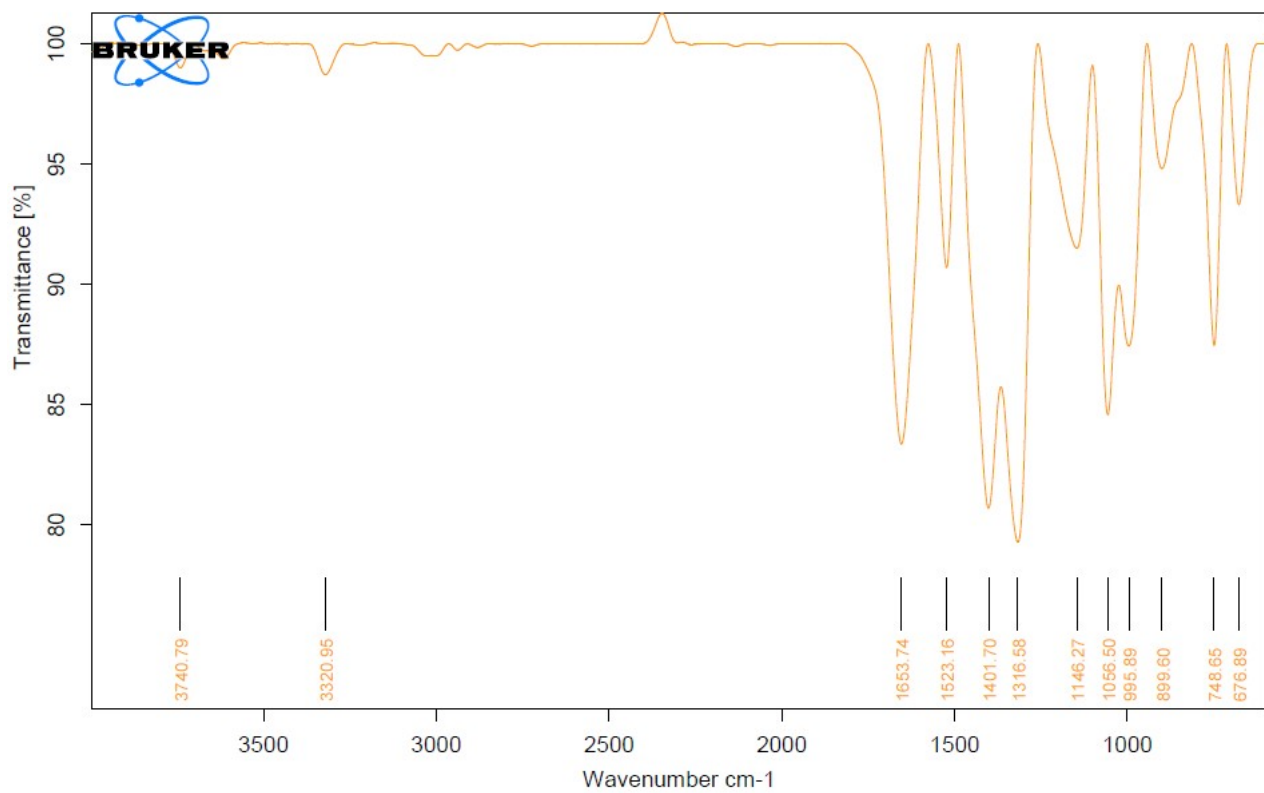


Fig.S28: IR Spectrum of Compound 5.

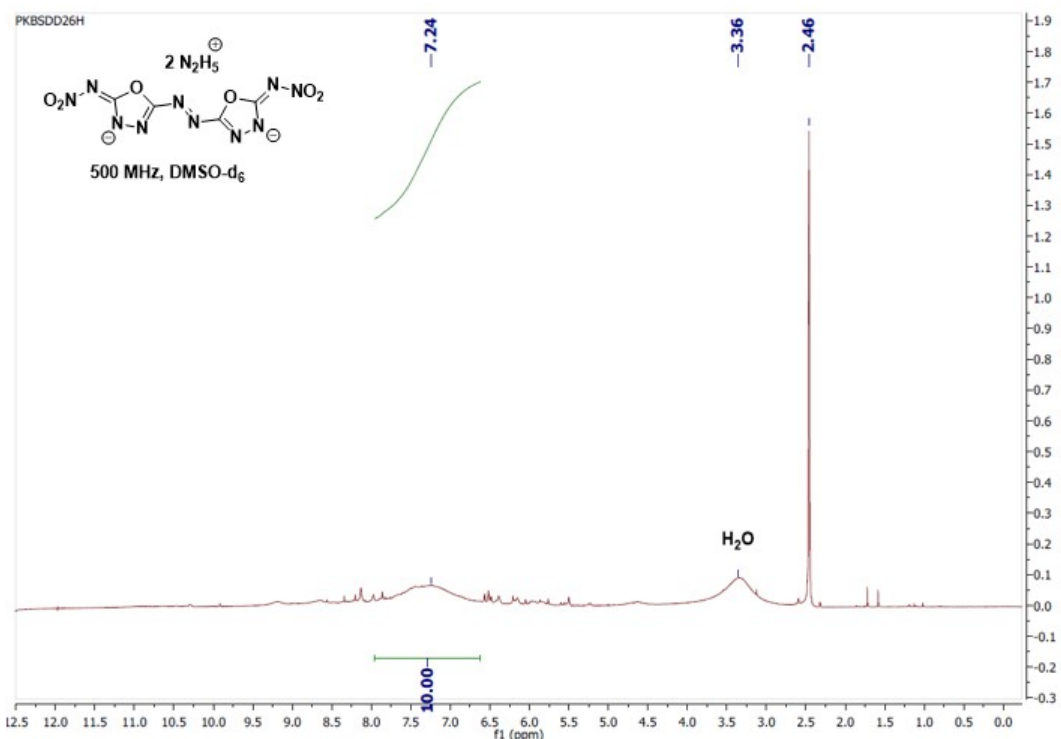


Fig.S29: ^1H NMR Spectra of Compound 6

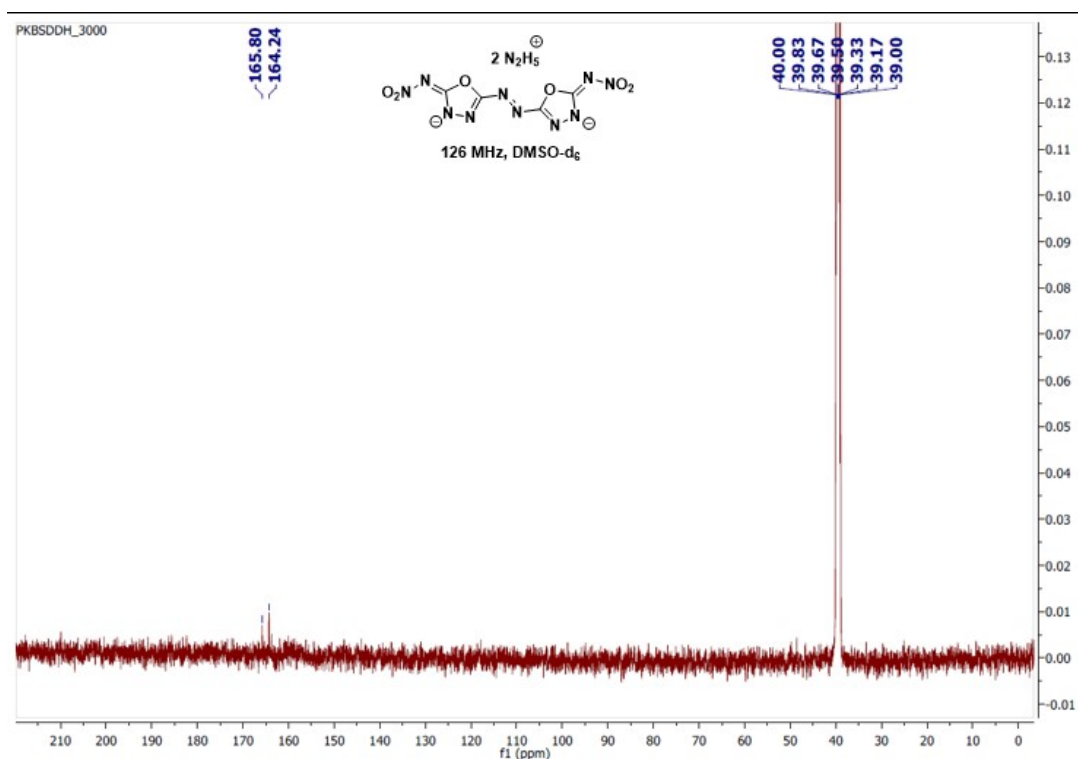


Fig.S30: ^{13}C NMR Spectra of Compound 6

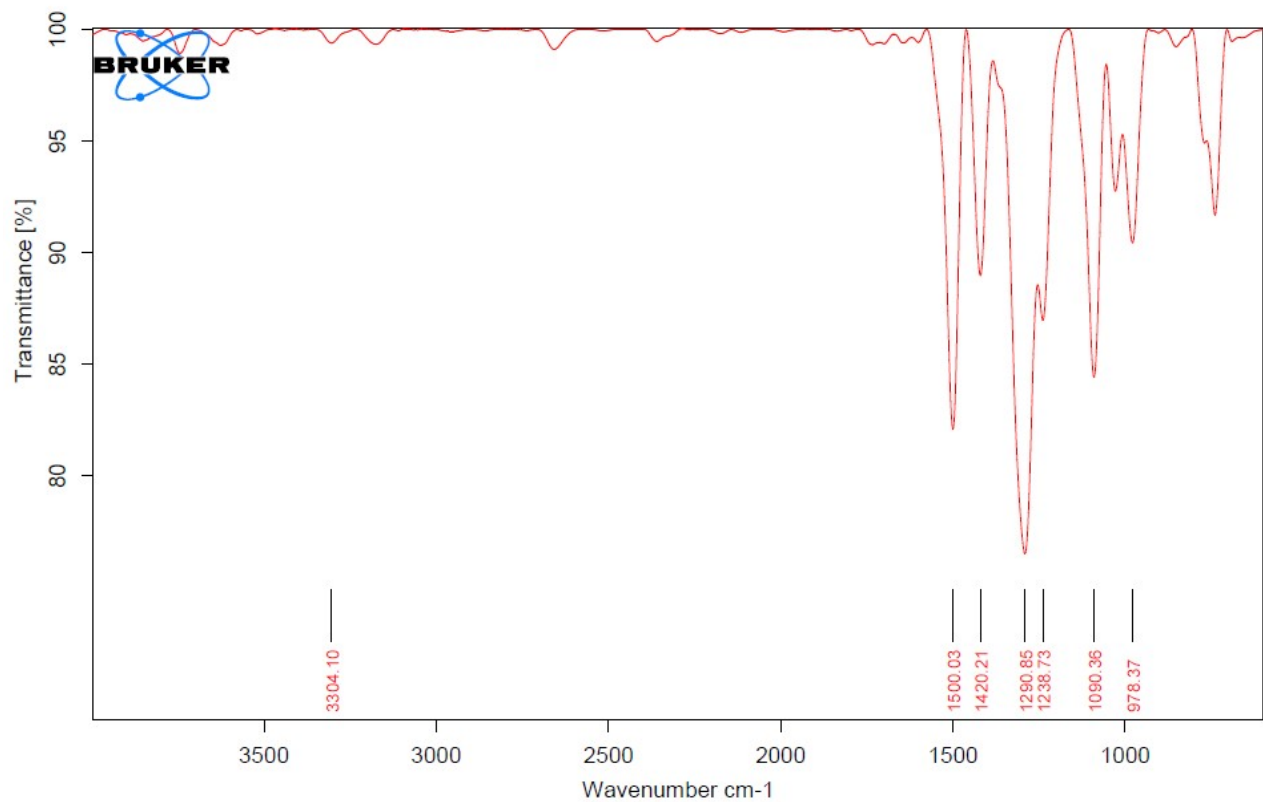


Fig.S31: IR Spectrum of Compound 6.

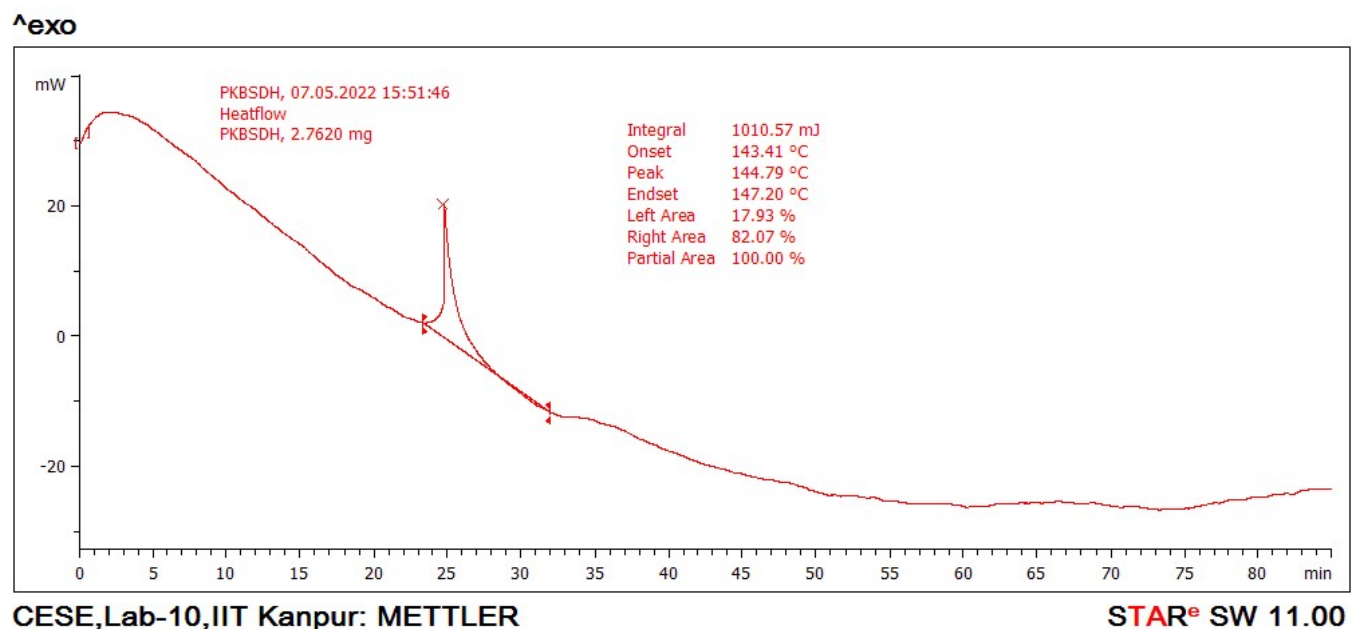


Fig S32. DSC Plot of Compound 6 at the Heating rate 5 °C min⁻¹.

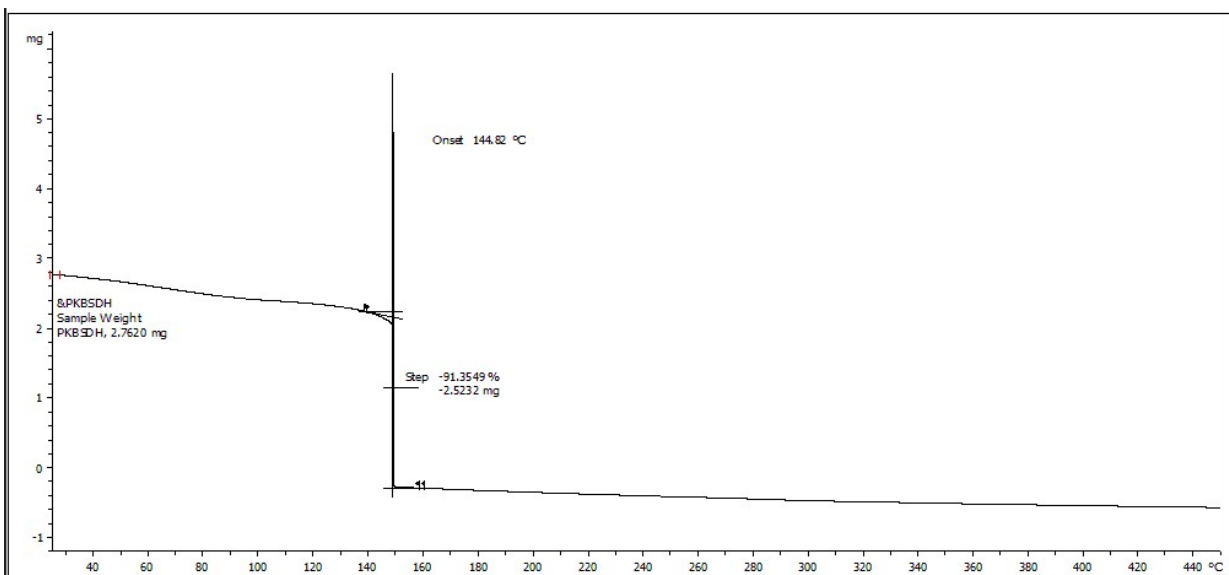


Fig S33. TGA curve of Compound 6 at the Heating rate 5 °C min⁻¹.

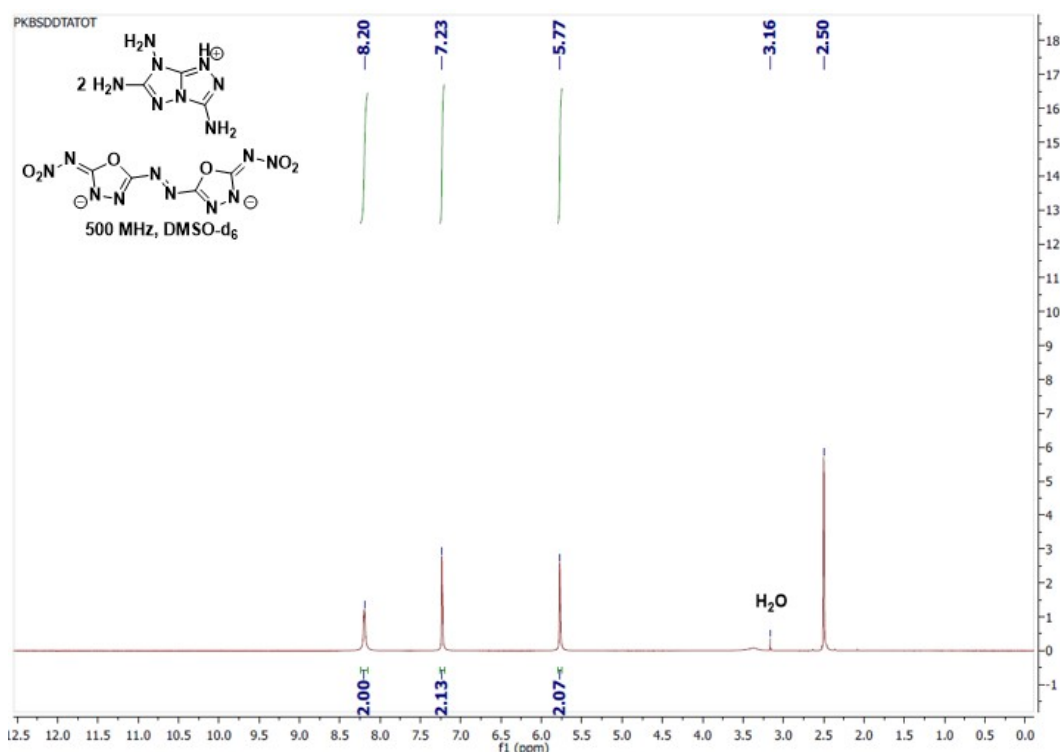


Fig.S34: ¹H NMR Spectra of Compound 7

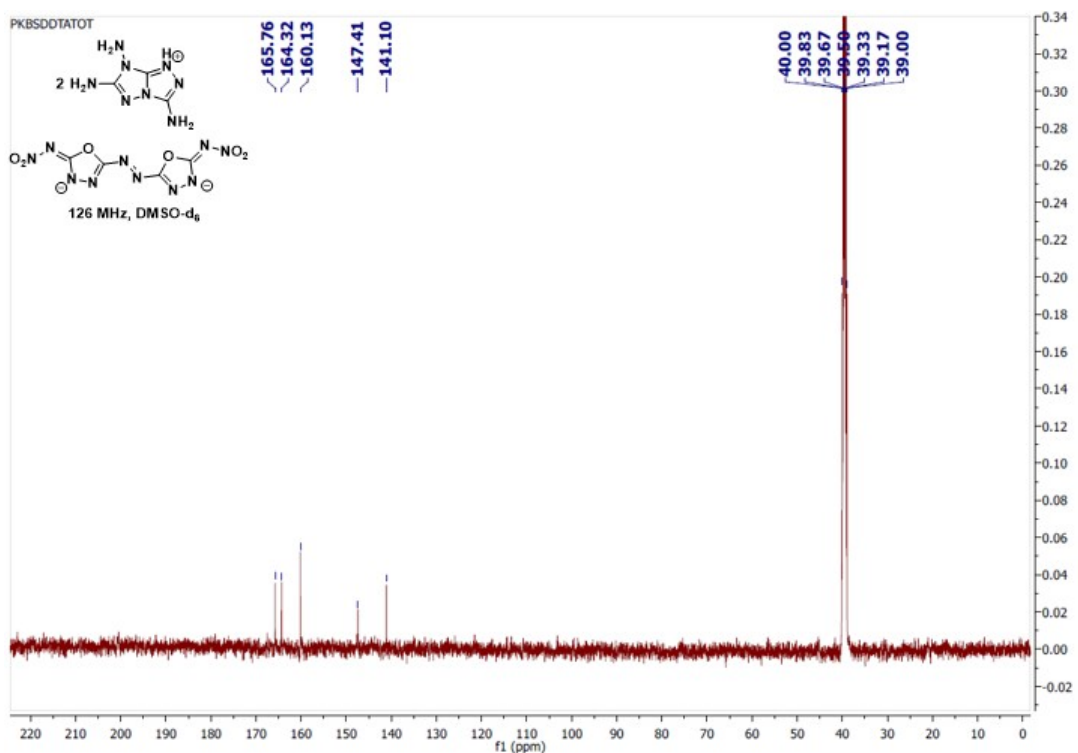


Fig.S35: ^{13}C NMR Spectra of Compound 7

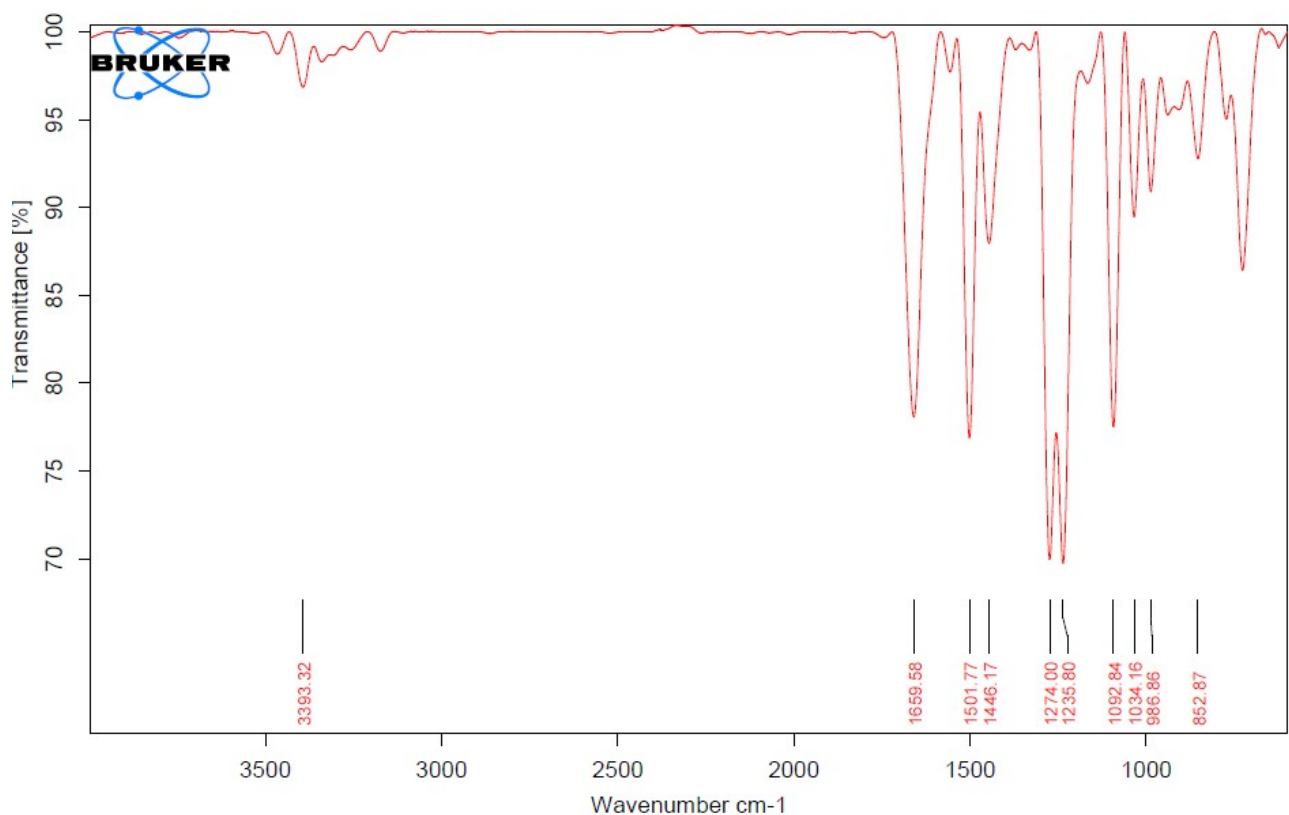
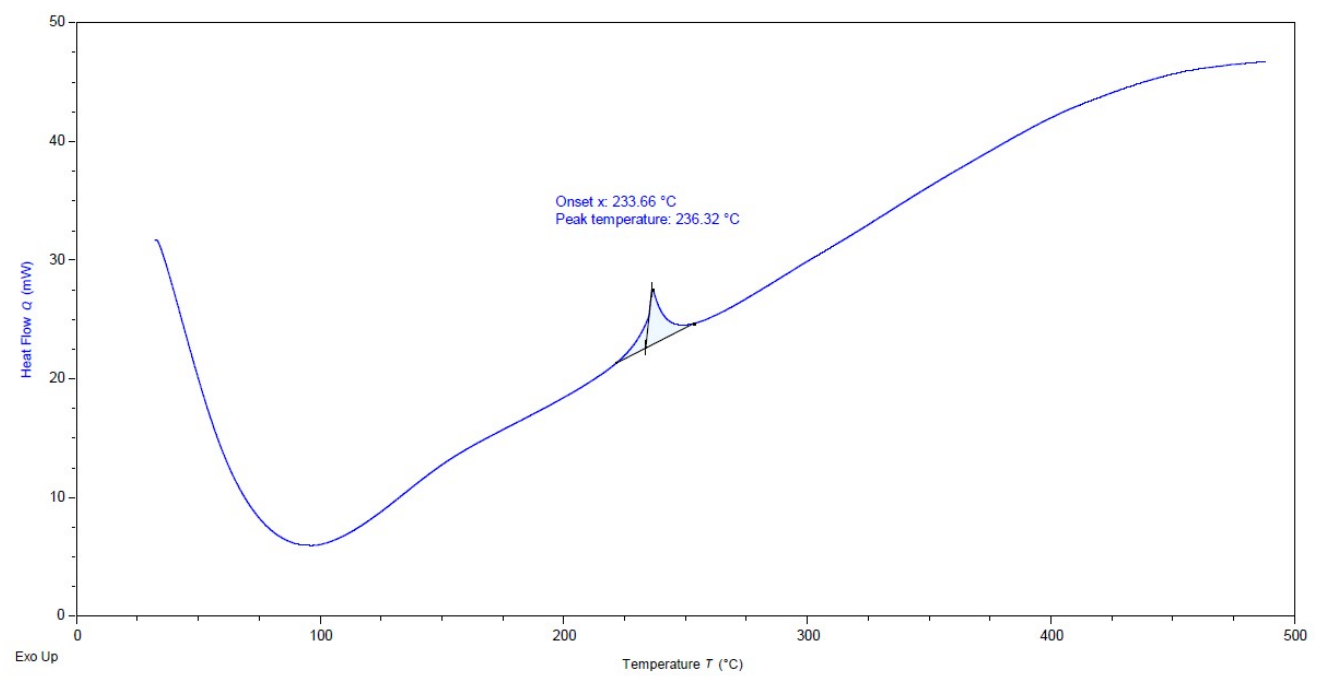
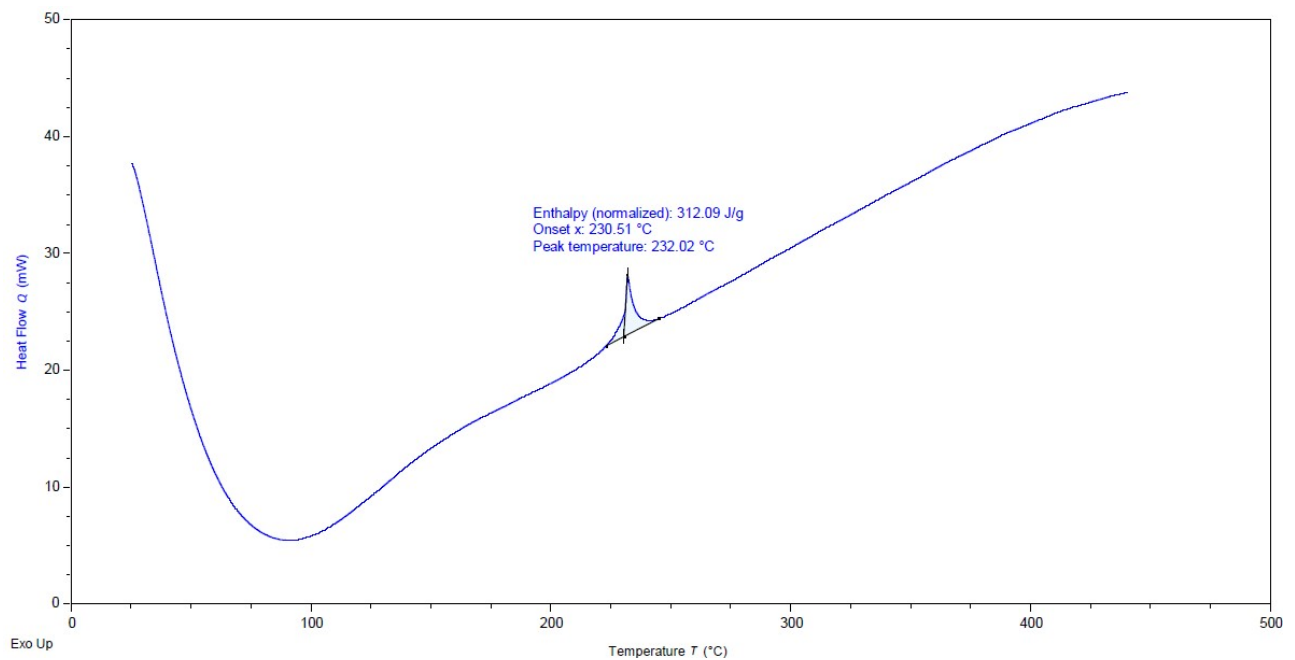
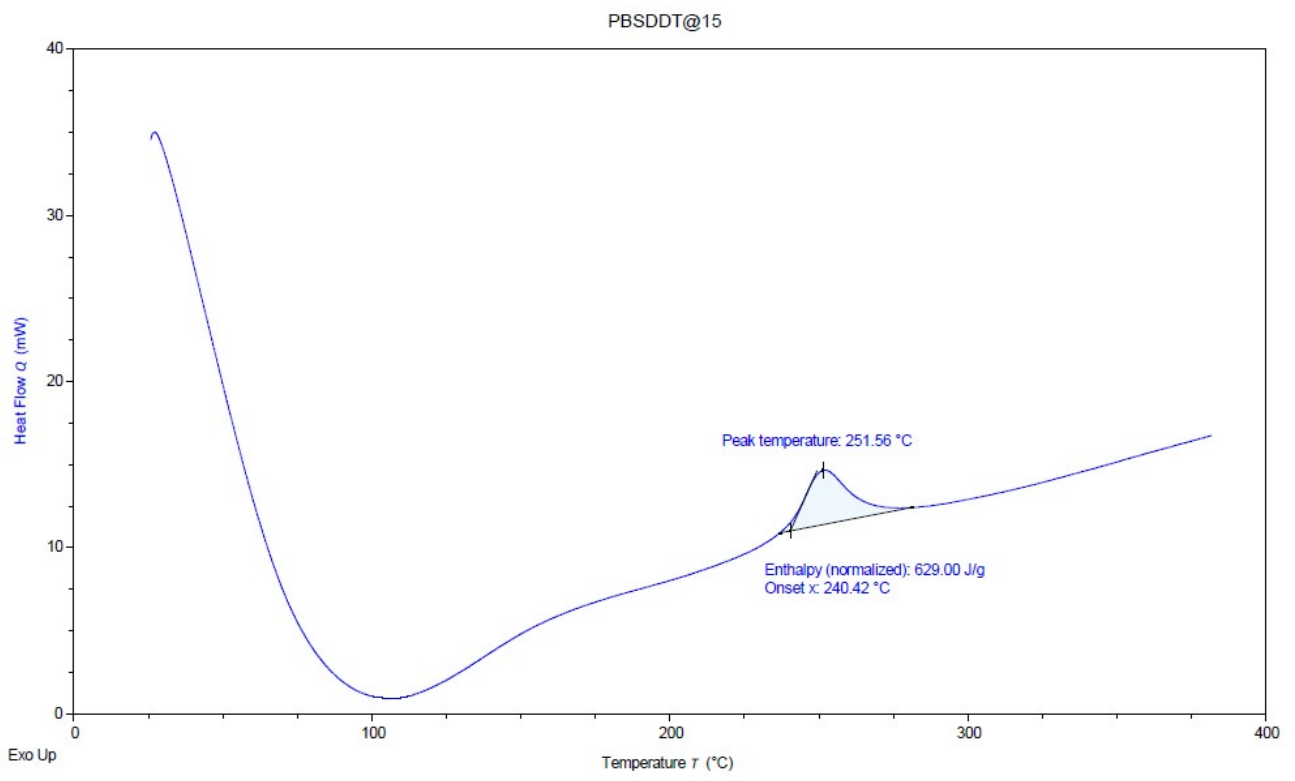


Fig.S36: IR Spectrum of Compound 7.





TA Instruments Trios V5.5.0.323

Fig S37. DSC Plot of Compound 7 at the Heating rate 5, 10 and 15 $^{\circ}\text{C min}^{-1}$ respectively.

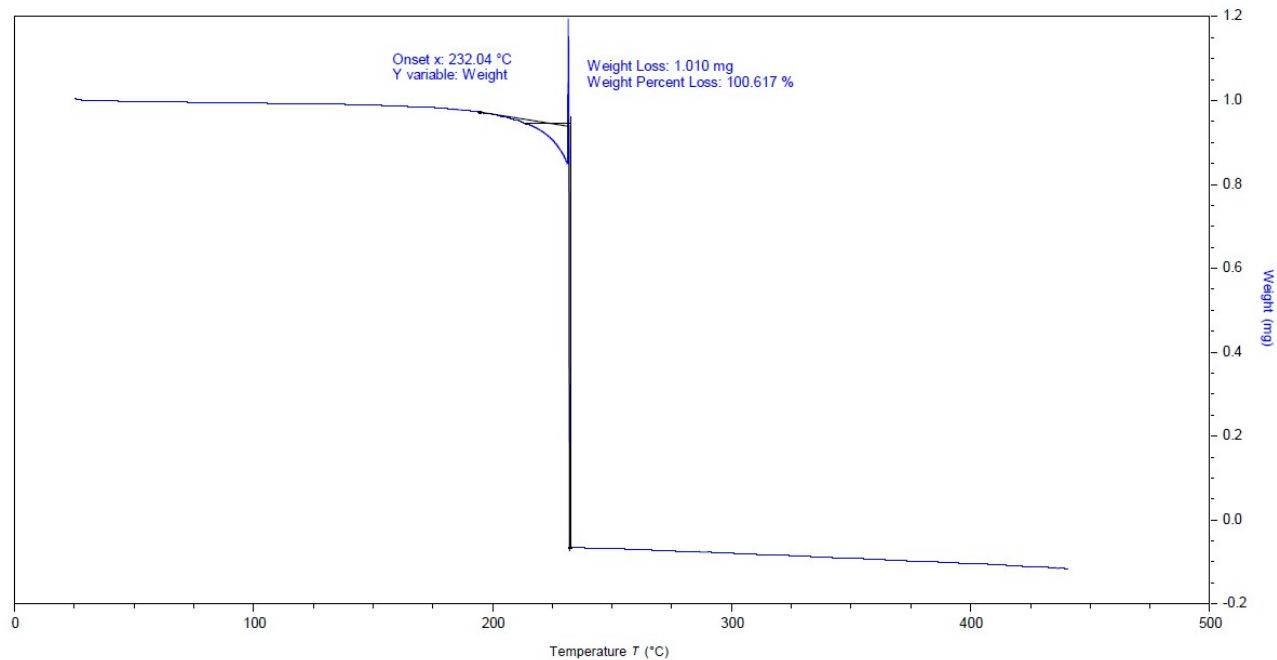


Fig S38. TGA Curve of Compound 7 at the Heating rate 5 $^{\circ}\text{C min}^{-1}$.

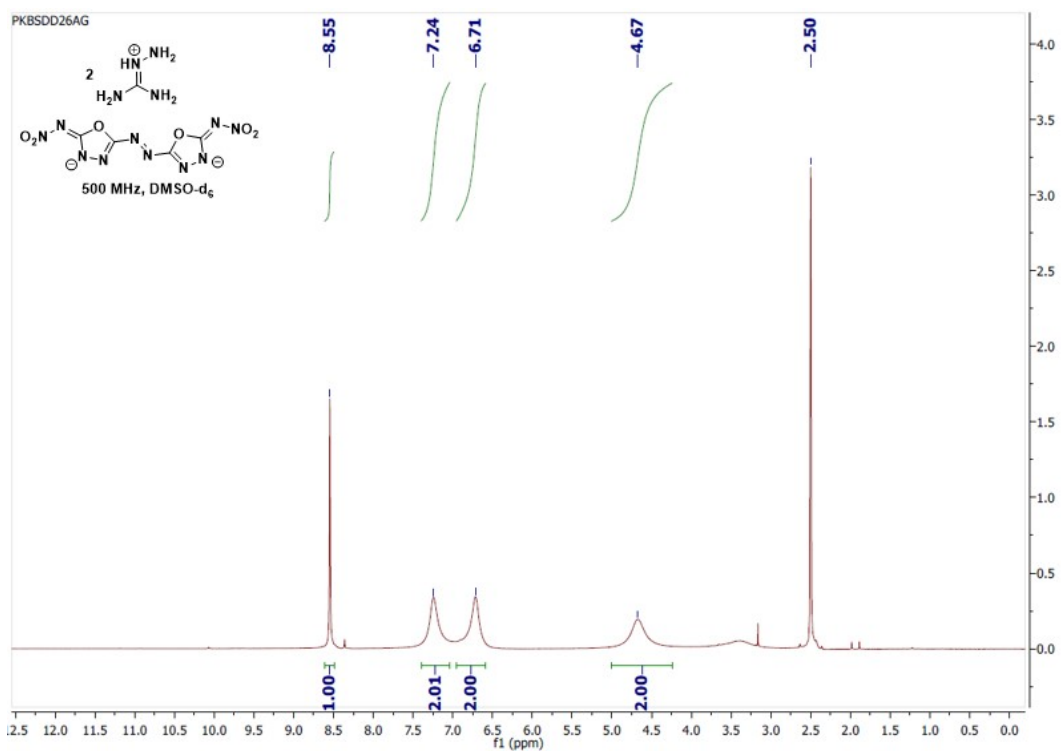


Fig.S39: ^1H NMR Spectra of Compound 8

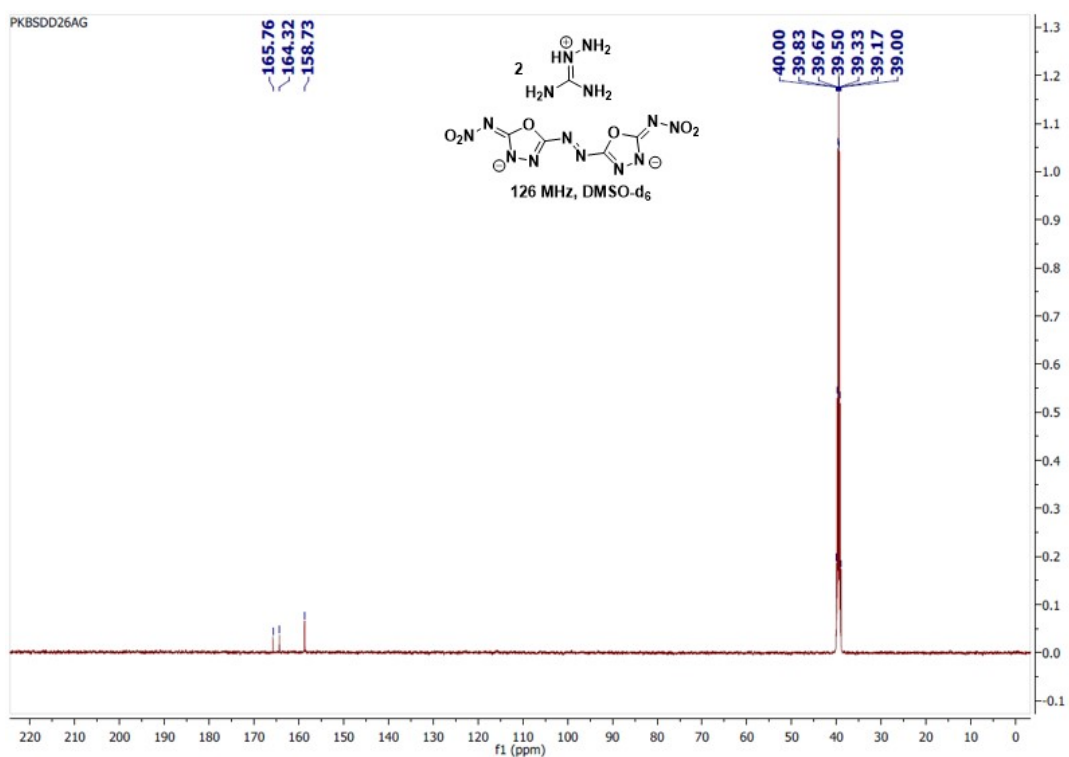


Fig.S40: ^{13}C NMR Spectra of Compound 8

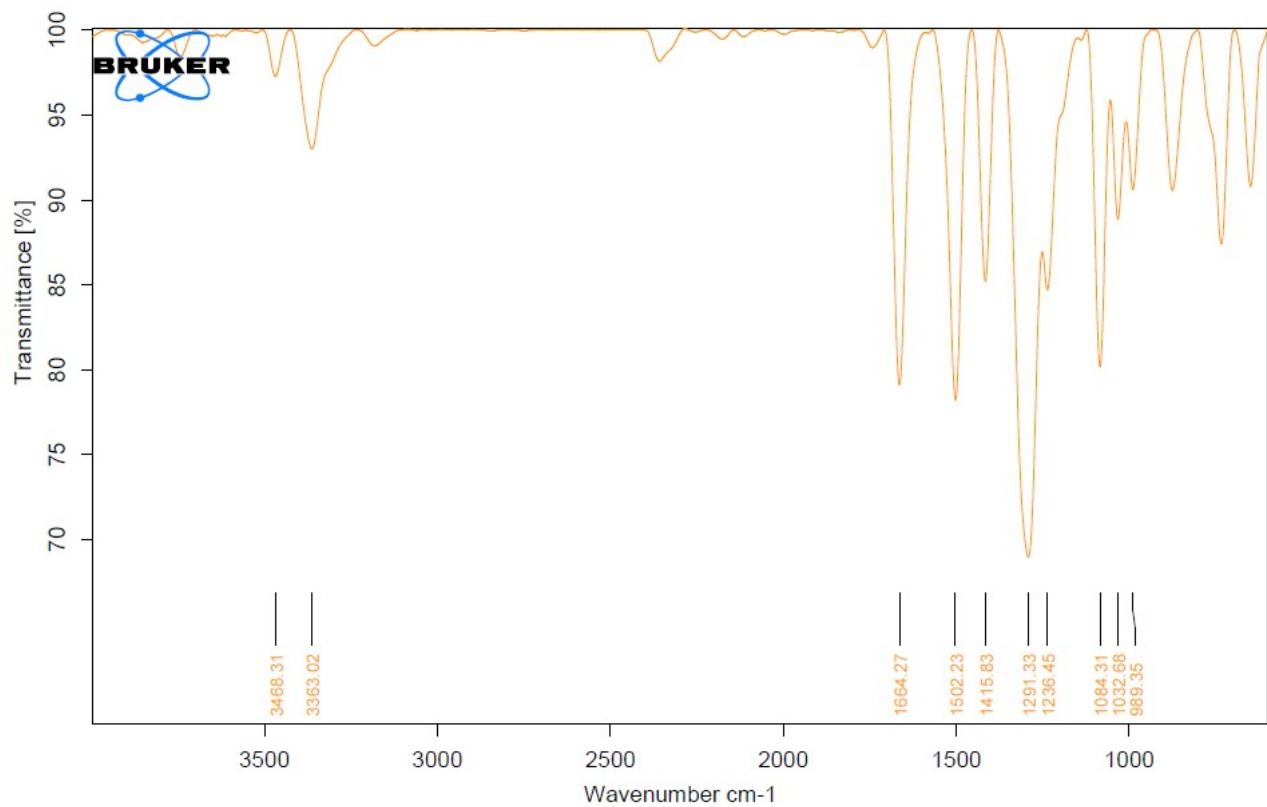
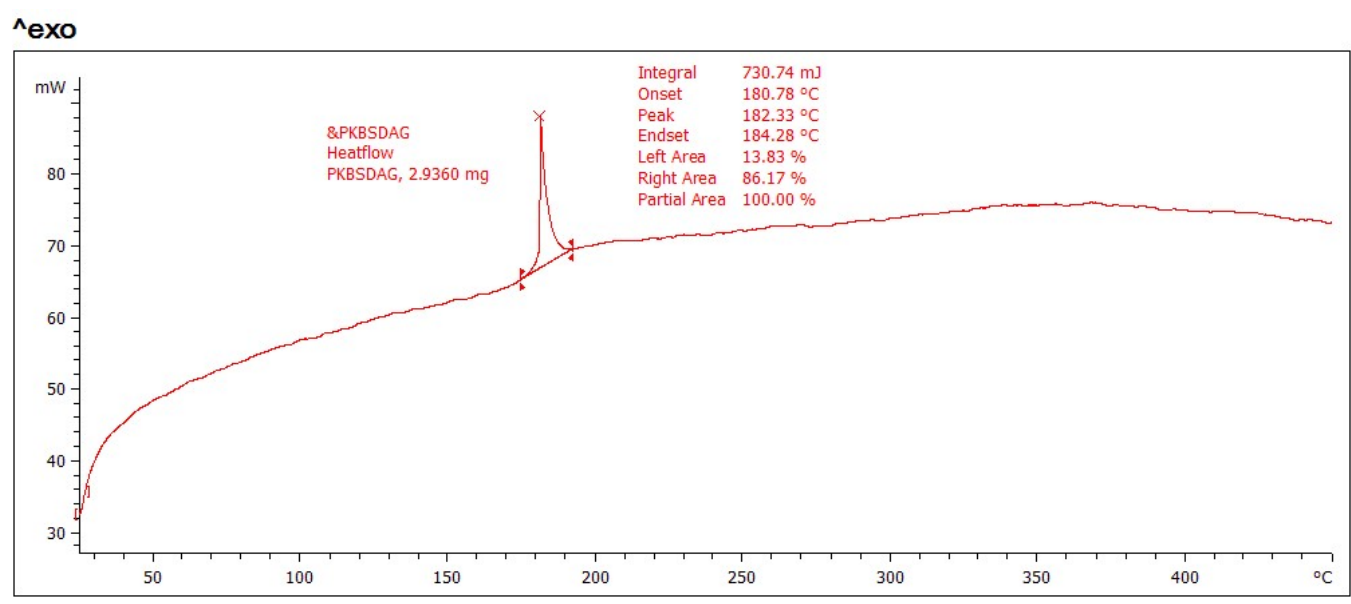


Fig.S41: IR Spectrum of Compound 8.



CESE,Lab-10,IIT Kanpur: METTLER

STAR^e SW 11.00

Fig S42. DSC Plot of Compound 8 at the Heating rate $5 \text{ }^{\circ}\text{C min}^{-1}$.

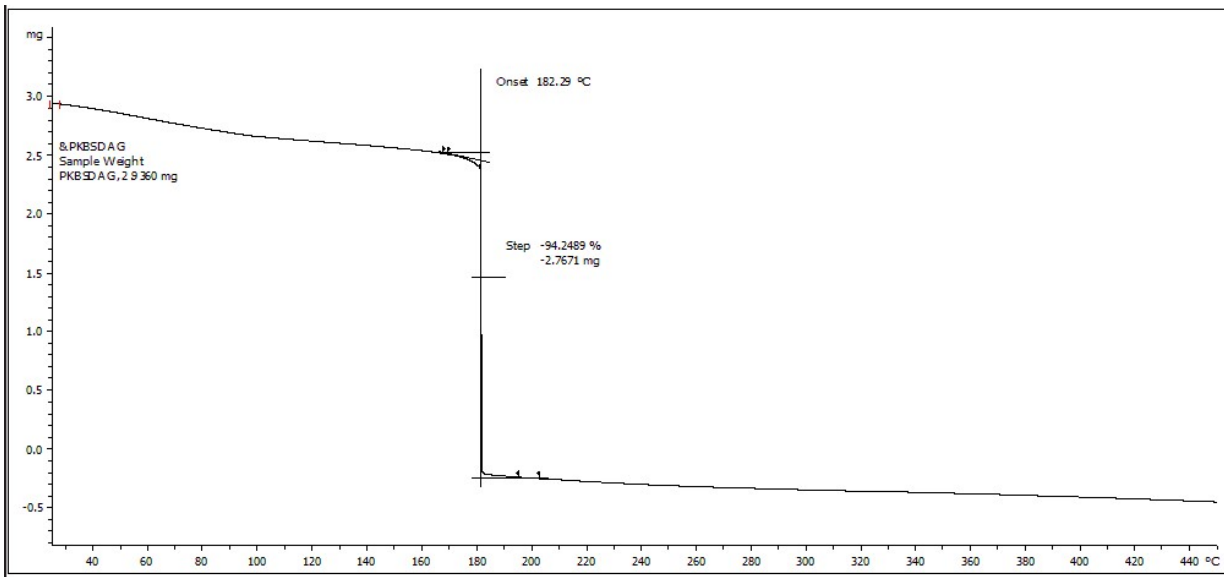


Fig S43. DSC Plot of Compound 8 at the Heating rate 5 °C min⁻¹.

Computational Details

Computations were carried out using the Gaussian 09 program suite.¹ The structure optimizations are performed with B3PW91 functional with 6-31G(d,p) basis set and characterized to be true local energy minima on the potential energy surface and no imaginary frequencies were found. Isodesmic reactions have been designed to predict the gas phase HOF (HOF_{gas}) and shown in Figure S44. The total energies (E_0), zero point correction (ZPE), thermal corrections (H_T), and the experimental/calculated HOF values of the reference compounds used in isodesmic reactions and other derivatives are given in Table S24 and S25. The usage of HOF_{gas} in the calculation of detonation properties slightly overestimates the values of detonation velocity and detonation pressure, and hence, the solid phase HOF ($\text{HOF}_{\text{solid}}$) can effectively reduce the errors. The $\text{HOF}_{\text{solid}}$ is calculated as the difference between HOF_{gas} and heat of sublimation (HOF_{sub}) as,

$$\text{HOF}_{\text{solid}} = \text{HOF}_{\text{gas}} - \text{HOF}_{\text{sub}} \quad (1)$$

HOF_{sub} depend on the molecular surface properties and calculated using equation (2) proposed by Politzer et al.,²

$$\text{HOF}_{\text{sub}} = 4.4307 \times 10^{-4} A^2 + 2.0599(v\sigma_{\text{tot}}^2)^{0.5} - 2.4825 \quad (2)$$

where A represent the surface area of the 0.001 electrons/bohr³ isosurface of electronic density, v denotes the degree of balance between the positive and negative surface potentials, and σ_{tot}^2 is the electrostatic potential variance. The molecular surface properties (see Table S26) were obtained using the Multiwfnn program.³ The gas-phase heats of formation (HOF_{gas}) of nitrate, perchlorate, and azide anions were calculated by G4 theory. The HOF_{gas} of picrate anion was obtained from previous reports.⁴ the HOF of energetic salts were predicted using Born–Haber cycle (Figure S45) and can be simplified by the equation (3),

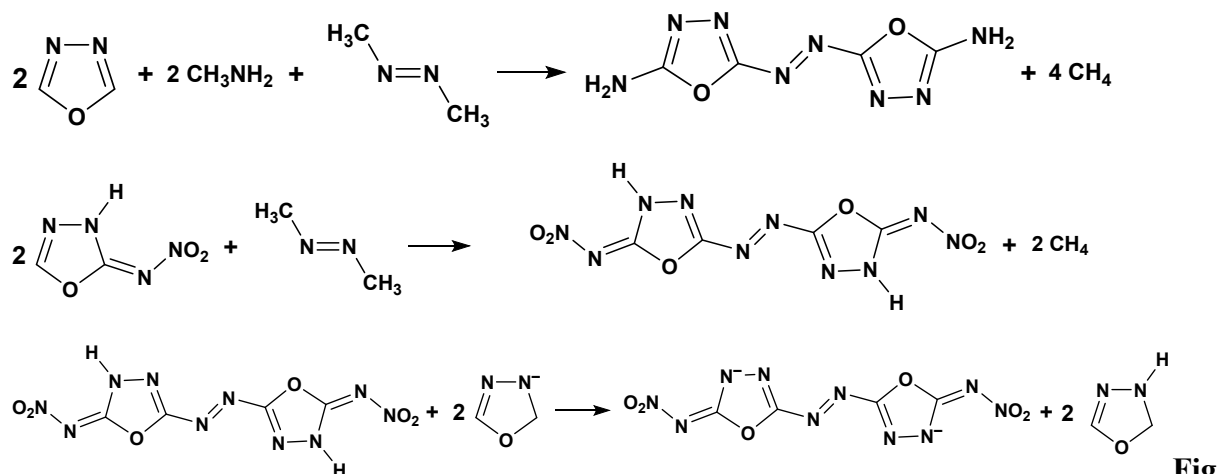
$$\text{HOF (salt, 298 K)} = \text{HOF (cation, 298 K)} + \text{HOF (anion, 298 K)} - H_L \quad (3)$$

in above equation, H_L is the lattice energy of the salts (see Table S27), which can be predicted by using the formula proposed by Jenkins et al.⁵

$$H_L = U_{\text{POT}} + [p(\frac{n_M}{2} - 2) + q(\frac{n_X}{2} - 2)]RT \quad (4)$$

The nature of the cation M_p^+ and anion X_q^- decide n_M and n_X values, respectively and are equal to three for monoatomic ions, five for linear polyatomic ions, and six for nonlinear polyatomic ions. U_{POT} is the lattice potential energy, calculated using the density (ρ in g/cm³) and the chemical formula mass (M in g/mol) of the ionic salt by the formula given in the following equation:

$$U_{\text{POT}} = 1981.2(\frac{\rho}{M})^{1/3} + 103.8 \quad (5)$$



Fig

ure S44. Designed isodesmic reactions for the prediction of HOF_{gas} of compound **4**, **5**, and anion of compound **5**.

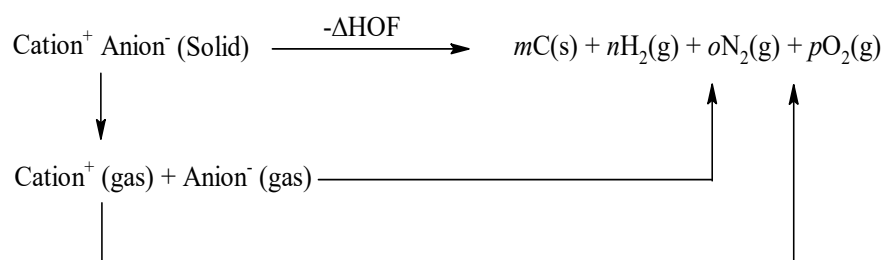
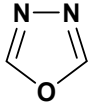
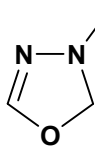
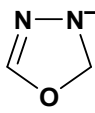
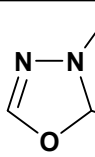


Figure S45. Born-Haber cycle for the formation of energetic salts.

Table S24. Calculated total energies at 298K (E_0), zero point energies (ZPE), and thermal corrections (H_T) and experimental HOF_{gas} of reference compounds used isodesmic reaction at the B3PW91/6-31G(d,p) level.

Compd.	E_0 (a.u.)	ZPE (au)	H_T (au)	HOF_{gas} (kJ/mol)
$\text{CH}_3\text{N}=\text{NCH}_3$	-189.119066	0.0847	0.006	152.66
CH_3NO_2	-244.866526	0.0502	0.0053	-81
	-261.945502	0.0468	0.0043	63.6
CH_3NH_2	-95.759911	0.0644	0.0043	-23.5
CH_4	-40.459807	0.045	0.0039	-74.8
	-263.115665	0.0702	0.0052	50.94
	-262.507656	0.0535	0.0052	65.84
	-521.666459	0.0671	0.0076	111.88

^aCalculated using G4 method.

Table S25. Calculated total energies at 298K (E_0), zero point energies (ZPE), and thermal corrections (H_T) and experimental HOF_{gas} of target compounds at the B3PW91/6-31G(d,p) level.

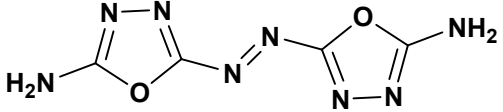
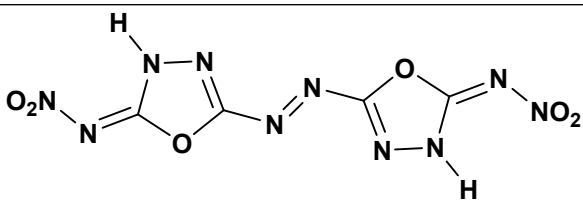
Compd.	E_0 (a.u.)	ZPE (au)	H_T (au)
	-742.773222	0.1151	0.0119
	- 1151.541143	0.1226	0.0167

Table S26. Calculated molecular surface properties and heat of sublimation of target compounds.

Compd.		Surfac e area (Å ²)	Volum e (Å ³)	σ_{tot}^2 (kcal/mol) ²	v	HOF _{Sublimat} ion (kJ/mol)
		206.12	193.30	457.37	0.2372	131.84
		263.67	252.54	357.77	0.1747	144.73

Table S27. Energy content of salts **6–8**.

Salt	HOF _c ^a	HOF _a ^b	U _{Pot} ^c	H _L ^d	HOF _{salt} ^e
6	769.5	179.45	1285.29	1297.68	420.8
7	1112.0	179.45	1042.02	1054.41	1349.0
8	671.7	179.45	1148.05	1160.44	362.4

^aHeat of formation of cation (kJ mol⁻¹). ^bHeat of formation of anion (kJ mol⁻¹). ^cLattice potential energy (kJ mol⁻¹). ^dLattice energy (kJ mol⁻¹). ^eHeat of formation of salt (kJ mol⁻¹).

In energetic materials, generally, C–NO₂, N–NO₂ and O–NO₂ are the weakest bond which easily ruptures on applying external stimuli. Hence, we have calculated the bond dissociation energy (BDE) of longest C–NO₂, N–NO₂ or O–NO₂ bond using following equation (6) at B3PW91/6-31G(d,p) level,

$$BDE = [E_{R1} + E_{R2}] - E_{R1-R2} \quad (6)$$

where E_{R1-R2}, E_{R1} and E_{R2} are the total energies with zero point energy correction of the precursor and the corresponding radicals produced by bond dissociation (see Table S25). The calculated bond dissociation energies of N–NO₂ bond in compound **5** and ICM-101 are shown in Figures S46 and S47.

Table S28. Calculated total energies (E₀) of R–NO₂, R, and NO₂ at the B3PW91/6-31G(d,p) level, used in the prediction of bond dissociation energies.

Compd.	E ₀ (a.u.)		
	R-NO ₂	R	NO ₂
5	-1151.541143	-946.482720	-204.982012

ICM-101	-1042.153955	-837.096414	-204.982012
---------	--------------	-------------	-------------

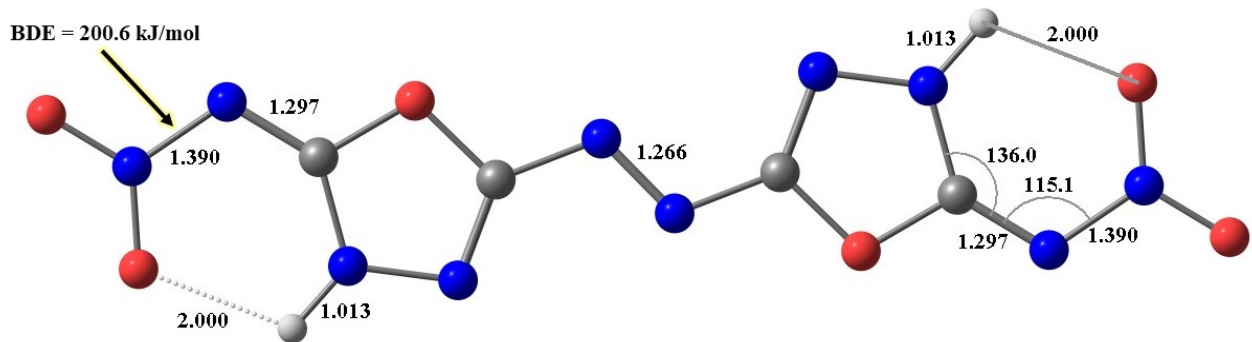


Figure S46. Selective bond lengths (\AA), angles ($^{\circ}$), and computed bond dissociation energy of N-NO₂ bond in compound **5**.

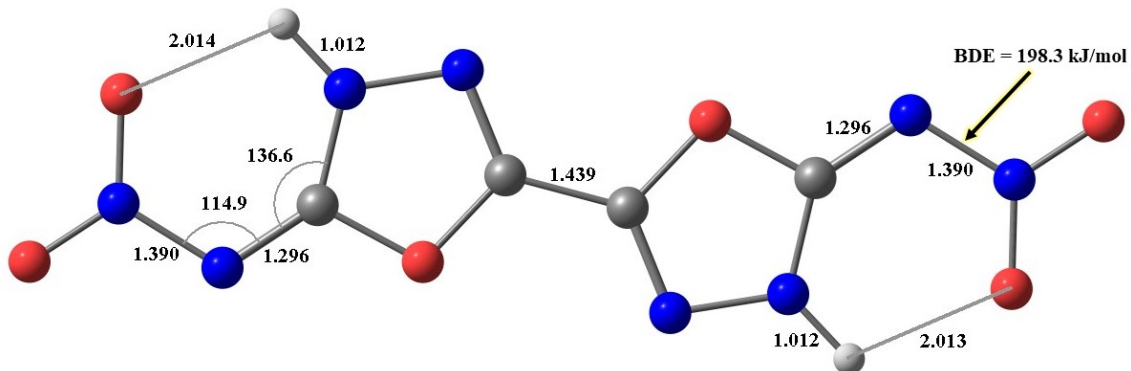
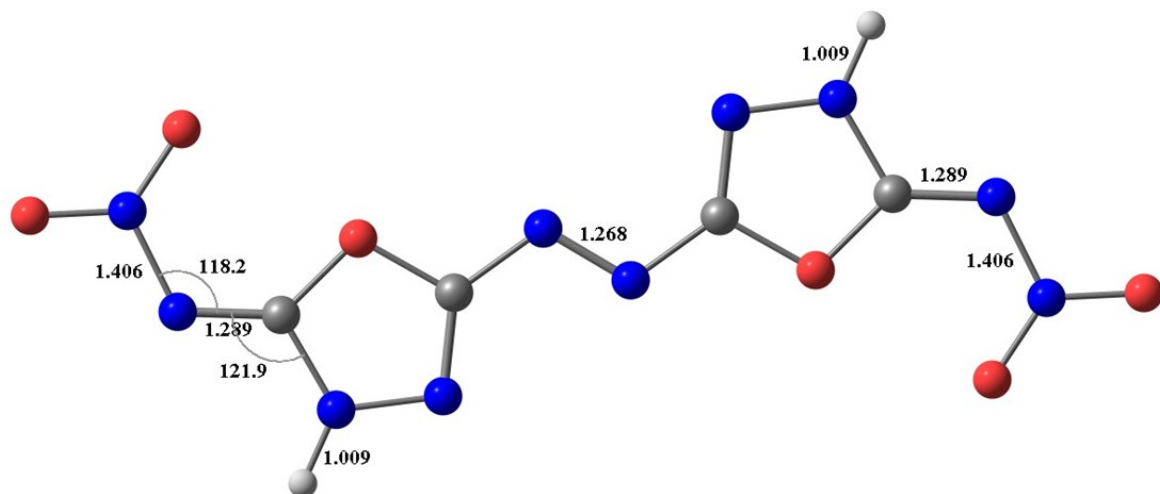


Figure S47. Selective bond lengths (\AA), angles ($^{\circ}$), and computed bond dissociation energy of N-NO₂ bond in compound ICM-101.

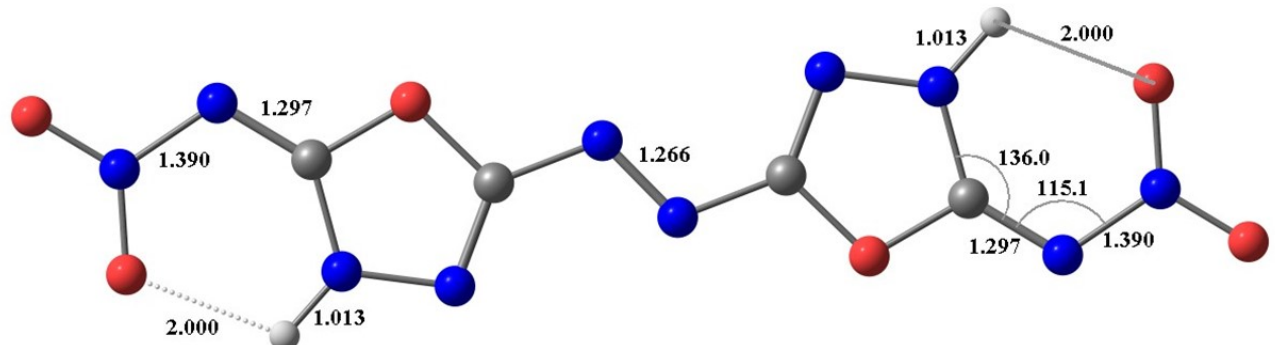
The relative stabilities of the geometrical isomers of compound **5** have been studied by DFT calculations.

Figures S48 and S49 represents the optimized structures of **5a** and **5b** isomers. As seen in Figure S49, the N-NO₂ group in these isomers was oriented to maximize internal hydrogen bonding and lowers the total energy. Compound **5b** forms a stable six membered H-bonded ring, which is absent in **5a**.



Energy: -1151.5231 Hartree (C1)

Figure S48. Optimized structure of compound 5 (named as 5a) where N-NO₂ group and N-H are away from each other.



Energy: -1151.5411 Hartree (C2)

Figure S49. Optimized structure of compound 5 (named as 5b) where N-NO₂ group and N-H are closer to each other.

Table S29. DSC data of compound **7** at various heating rates (Kissinger method).

Compd.	β (°C)	T_m (K)	T_m^2	$1/T_m$	β/T_m^2	$-\ln(\beta/T_m^2)$	R	Activation energy (kJ/mol)
7	5	514.2	264350.2	0.00194	1.8914×10^{-5}	-10.88	1	225.92
	10	520.8	271180.6	0.00192	3.6875×10^{-5}	-10.21		
	15	524.7	275257.6	0.00191	5.4494×10^{-5}	-9.82		

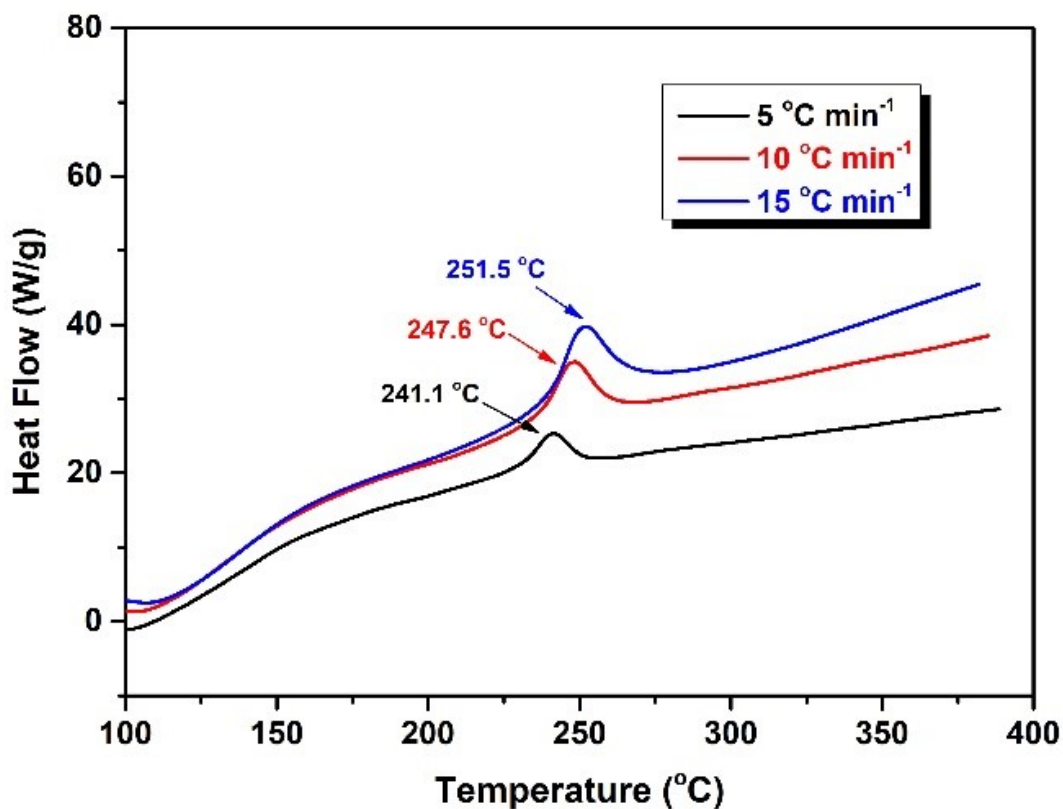


Figure S50. DSC curves of **7** at different heating rates.

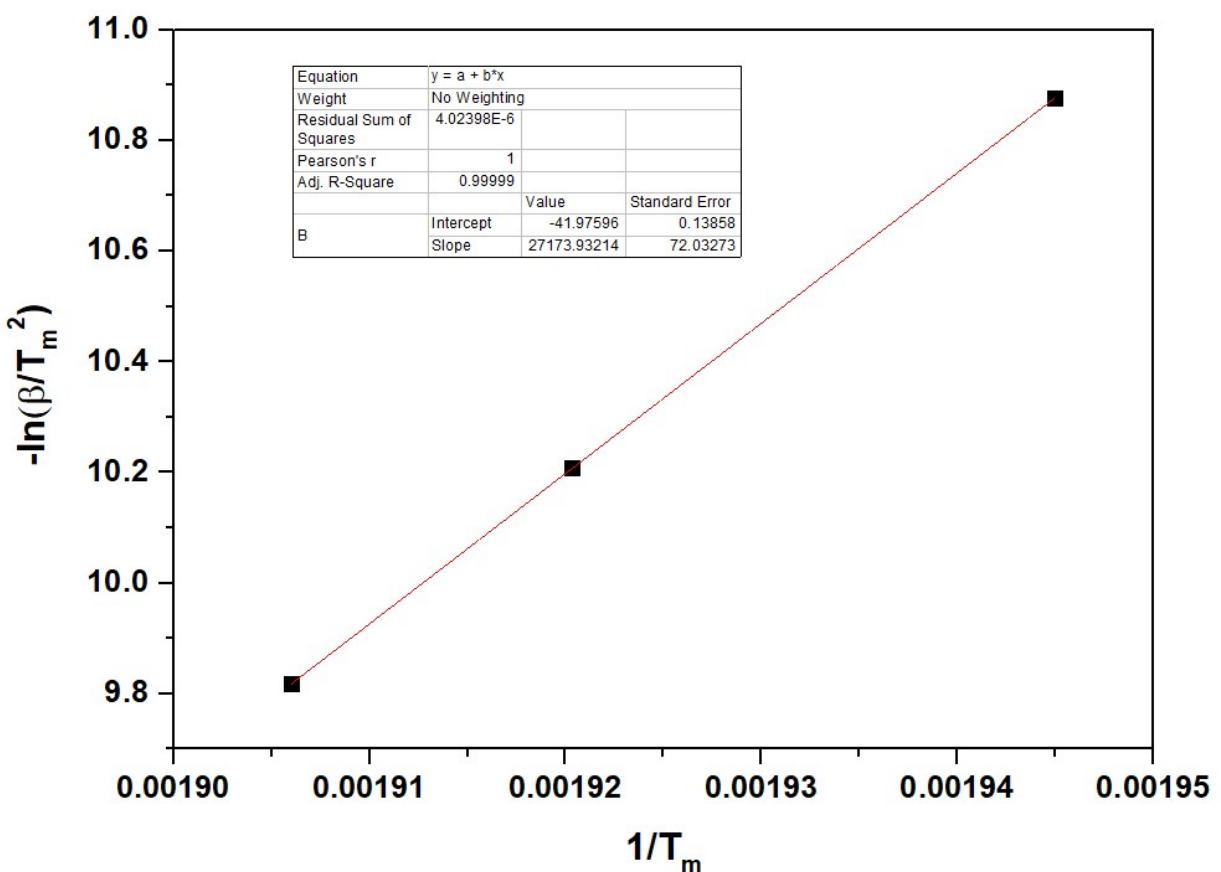


Figure S51. A plot of $1/T_m$ vs $-\ln(\beta/T_m^2)$ (Kissinger method) for compound 7.

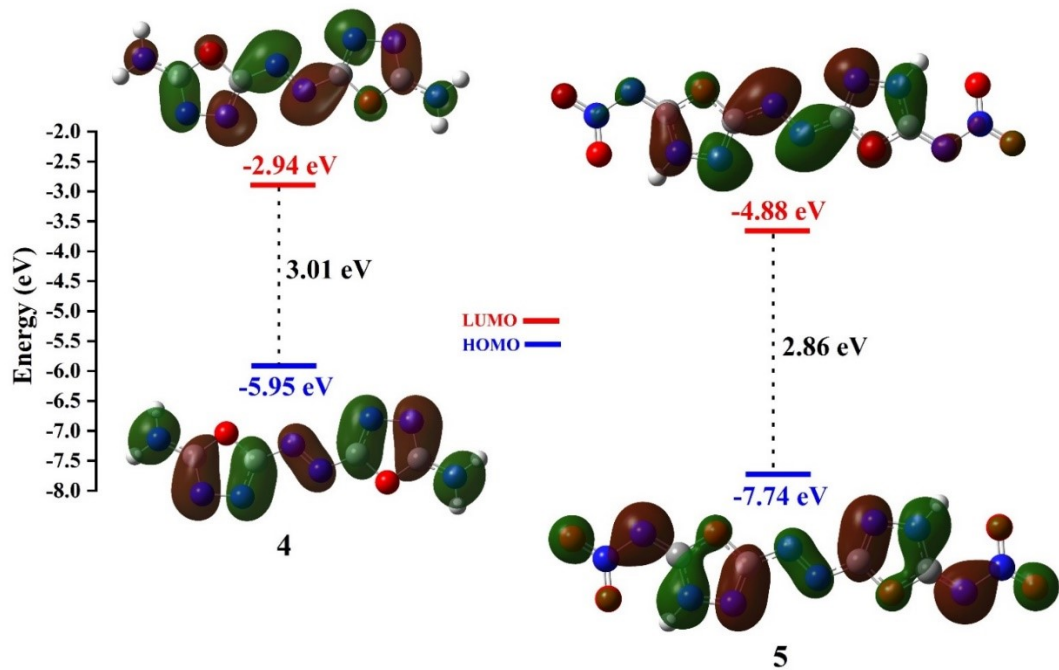


Fig. S52. Contour plots of the frontier orbitals of compounds 4 and 5.

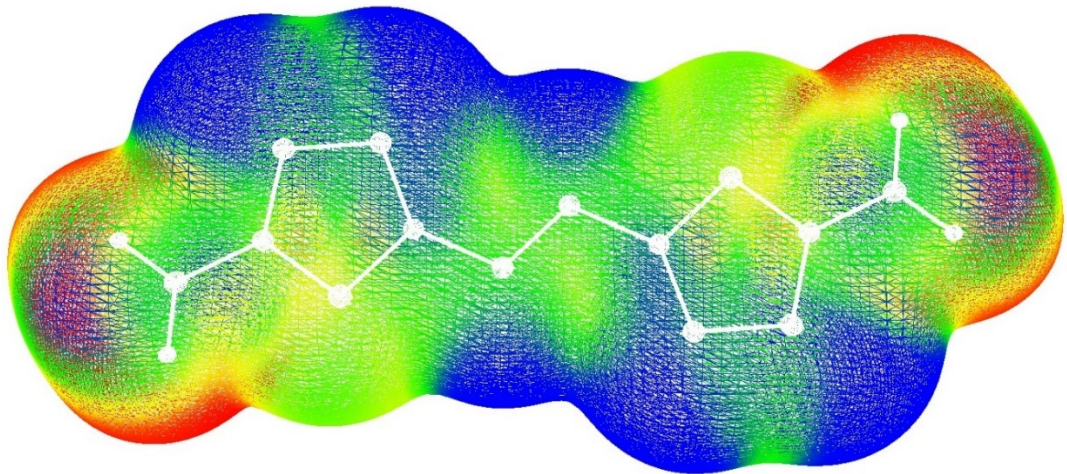


Figure S53. The electrostatic potentials for the 0.001 electron/bohr³ isosurfaces of electron density evaluated at the B3LYP level of theory for compound 4. (Color ranges for isosurface in kcal/mol, are: red > 15, yellow > 13, green > 11, blue < 11).

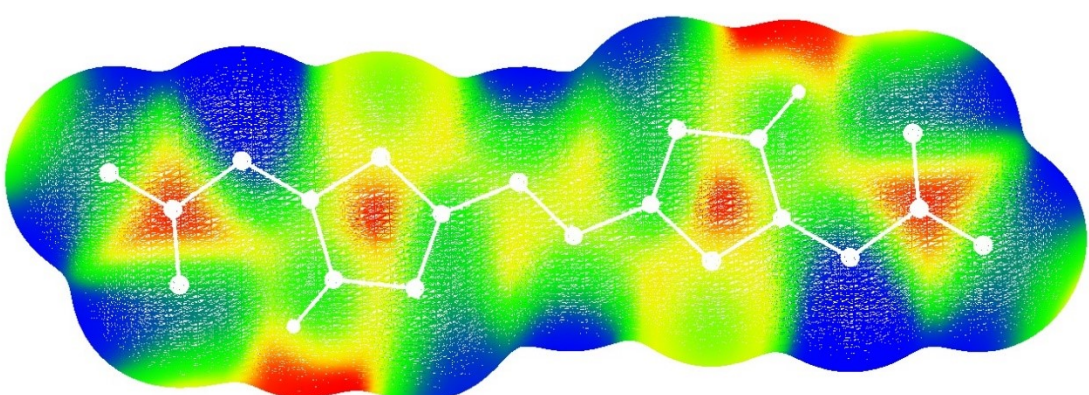


Figure S54. The electrostatic potentials for the 0.001 electron/bohr³ isosurfaces of electron density evaluated at the B3LYP level of theory for compound 5. (Color ranges for isosurface in kcal/mol, are: red > 16, yellow > 14, green > 12, blue < 12).

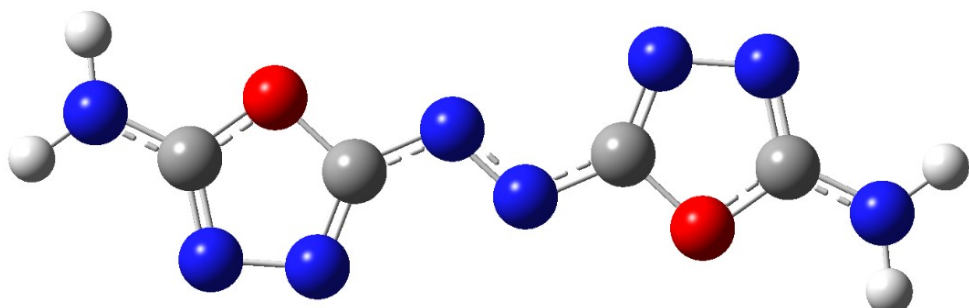


Figure S55. Optimized structure of compound 4 and its Cartesian coordinates at B3PW91/6-31G(d,p) level of theory

6	3.826897000	-0.056504000	-0.000036000
8	2.736525000	-0.831446000	-0.000219000
7	3.558149000	1.233040000	0.000268000
6	1.719931000	0.107432000	-0.000064000
7	2.193962000	1.323528000	0.000178000
7	0.467996000	-0.431553000	-0.000179000
7	-0.467996000	0.431552000	-0.000119000
6	-1.719931000	-0.107432000	-0.000075000
7	-2.193962000	-1.323529000	0.000105000
8	-2.736525000	0.831446000	0.000126000
7	-3.558149000	-1.233040000	0.000074000
6	-3.826897000	0.056504000	0.000027000
7	-5.035822000	0.639026000	-0.000233000
7	5.035823000	-0.639026000	-0.000506000
1	-5.851083000	0.051961000	0.000655000
1	-5.127569000	1.638772000	0.001092000
1	5.851082000	-0.051961000	0.001301000
1	5.127568000	-1.638772000	0.001462000

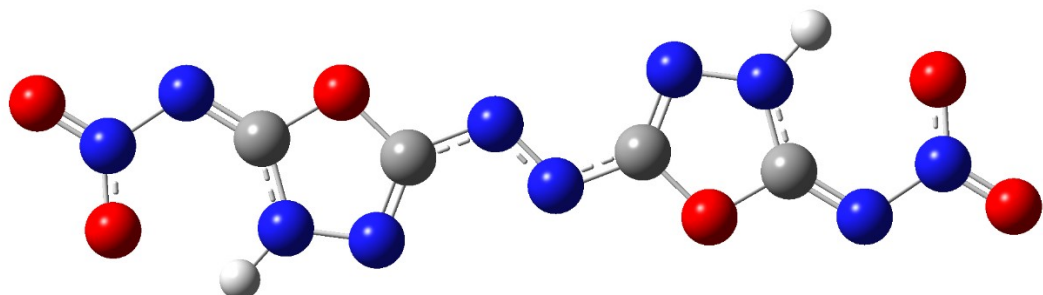


Figure S56. Optimized structure of compound **5** and its Cartesian coordinates at B3PW91/6-31G(d,p) level of theory.

6	-3.874739000	0.237960000	0.000110000
8	-2.703917000	0.914237000	0.000247000
7	-3.523128000	-1.077213000	-0.000146000
6	-1.724000000	-0.039013000	0.000067000

7	-2.187020000	-1.252707000	-0.000132000
7	-0.443438000	0.452068000	0.000357000
7	0.443429000	-0.451965000	-0.000343000
6	1.723990000	0.039109000	-0.000150000
7	2.187064000	1.252774000	-0.000332000
8	2.703895000	-0.914169000	-0.000055000
7	3.523151000	1.077258000	-0.000331000
6	3.874733000	-0.237940000	-0.000115000
7	4.986018000	-0.906826000	0.000010000
7	-4.986044000	0.906790000	0.000265000
1	-4.199387000	-1.831453000	-0.000148000
1	4.199349000	1.831534000	-0.000373000
7	6.140297000	-0.132937000	0.000170000
8	6.063815000	1.107497000	-0.000108000
8	7.177787000	-0.757545000	0.000517000
7	-6.140300000	0.132846000	0.000033000
8	-7.177821000	0.757404000	0.000052000
8	-6.063771000	-1.107597000	-0.000129000

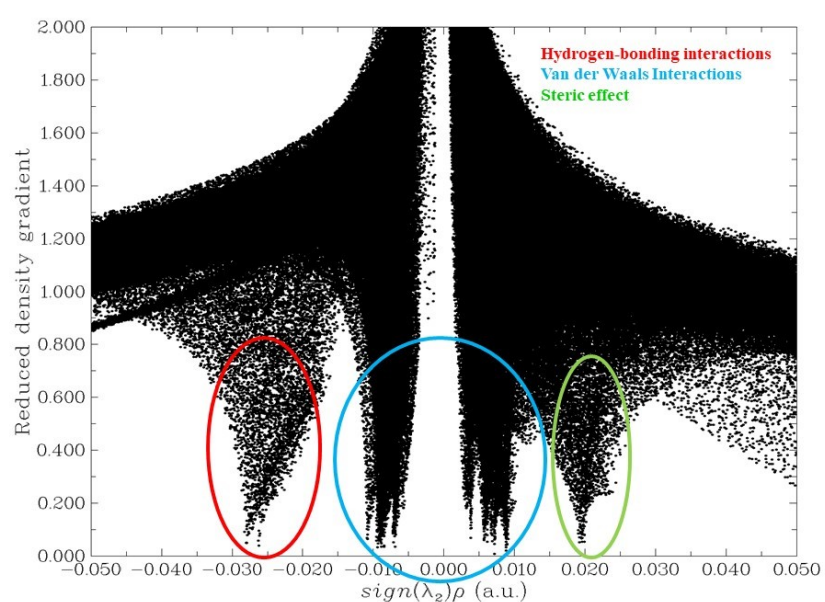


Figure S57. Scatter graph ($\text{sign}(\lambda_2)\rho$ vs RDG functions) for compound 5.

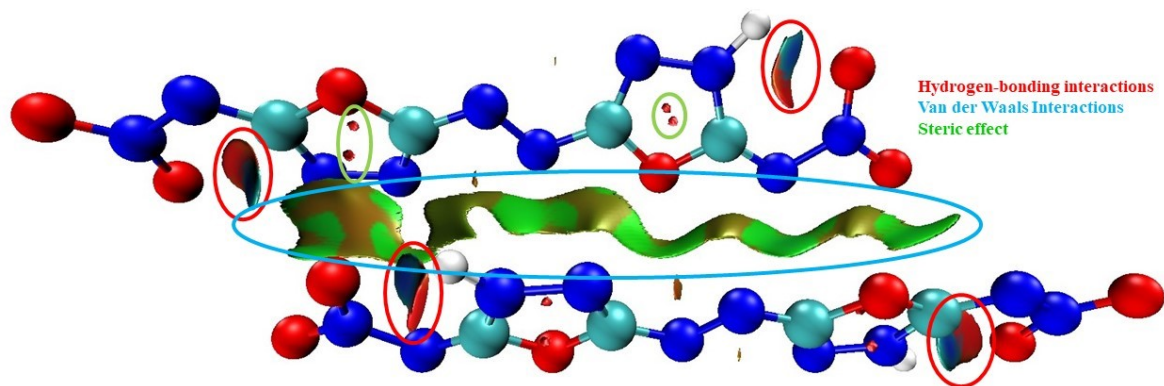


Figure S58. Reduced density gradient isosurface for compound **5**.

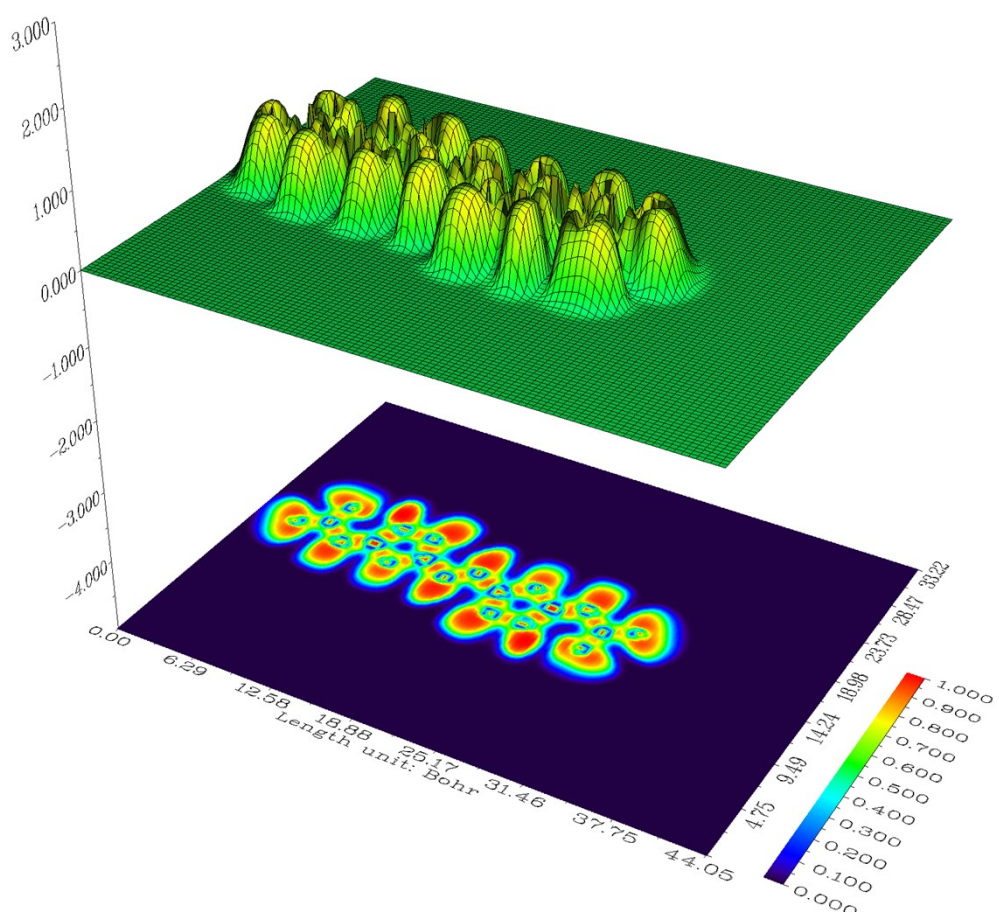


Figure S59. Surface map with projection effect of ELF of compound **5**.

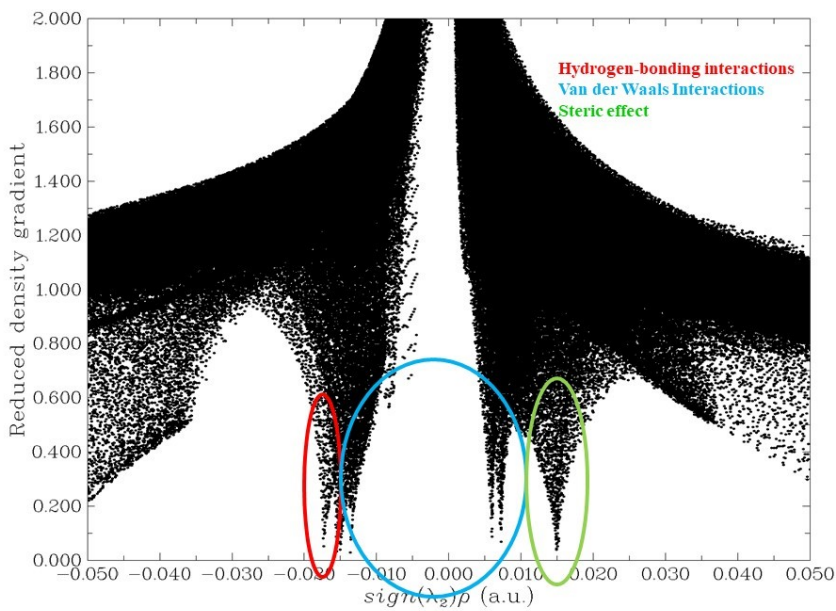


Figure S60. Scatter graph ($\text{sign}(\lambda_2)\rho$ vs RDG functions) for salt **6**.

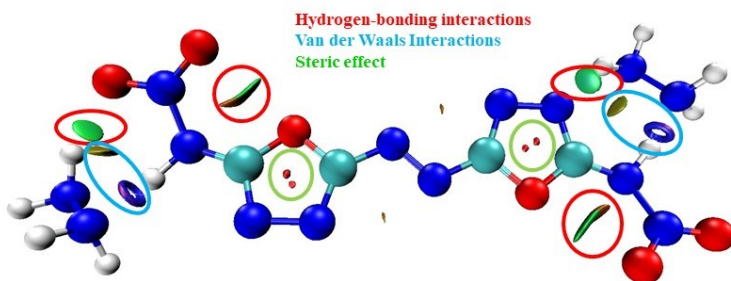


Figure S61. Reduced density gradient isosurface for salt **6**.

References

1. Gaussian 09, Revision E.01, M. J. Frisch, G. W. Trucks, H. B. Schlegel, G. E. Scuseria, M. A. Robb, J. R. Cheeseman, G. Scalmani, V. Barone, B. Mennucci, G. A. Petersson, H. Nakatsuji, M. Caricato, X. Li, H. P. Hratchian, A. F. Izmaylov, J. Bloino, G. Zheng, J. L. Sonnenberg, M. Hada, M. Ehara, K. Toyota, R. Fukuda, J. Hasegawa, M. Ishida, T. Nakajima, Y. Honda, O. Kitao, H. Nakai, T. Vreven, Jr. J. A. Montgomery, J. E. Peralta, F. Ogliaro, M. Bearpark, J. J. Heyd, E. Brothers, K. N. Kudin, V. N. Staroverov, R. Kobayashi, J. Normand, K. Raghavachari, A. Rendell, J. C. Burant, S. S. Iyengar, J. Tomasi, M. Cossi, N. Rega, J. M. Millam, M. Klene, J. E. Knox, J. B. Cross, V. Bakken, C. Adamo, J. Jaramillo, R. Gomperts, R. E. Stratmann, O. Yazyev, A. J. Austin, R. Cammi, C. Pomelli, J. W. Ochterski, R. L. Martin, K. Morokuma, V. G. Zakrzewski, G. A. Voth, P. Salvador, J. J. Dannenberg, S. Dapprich, A. D. Daniels, O. Farkas, J. B. Foresman, J. V. Ortiz, J. Cioslowski, D. J. Fox, *Gaussian, Inc.*, Wallingford CT, **2013**.
2. P. Politzer, Y. Ma, P. Lane, M. C. Concha, *Int J Quant Chem*, **105**, 341-347 (2005).
3. T. Lu, F. Chen, *J Comput Chem*, **3**, 580–592 (2012).

4. A. Devi, S. Dharavath, V. D. Ghule, *ChemistrySelect.*, **3**, 4501–4504 (2018).
5. H. D. B. Jenkins, D. Tudela, L. Glasser, Lattice Potential Energy Estimation for Complex Ionic Salts from Density Measurements, *Inorg. Chem.*, **41**, 2364 (2002).
6. Gaussian 09, Revision E.01, M. J. Frisch, G. W. Trucks, H. B. Schlegel, G. E. Scuseria, M A. Robb, J. R. Cheeseman, G. Scalmani, V. Barone, B. Mennucci, G. A. Petersson, H. Nakatsuji, M Caricato, X. Li, H. P. Hratchian, A. F. Izmaylov, J. Bloino, G. Zheng, J. L. Sonnenberg, M. Hada, M. Ehara, K. Toyota, R. Fukuda, J. Hasegawa, M. Ishida, T. Nakajima, Y. Honda, O. Kitao, H. Nakai, T. Vreven, Jr. J. A. Montgomery, J. E. Peralta, F. Ogliaro, M. Bearpark, J. J. Heyd, E. Brothers, K. N. Kudin, V. N. Staroverov, R. Kobayashi, J. Normand, K. Raghavachari, A. Rendell, J. C. Burant, S. S. Iyengar, J. Tomasi, M. Cossi, N. Rega, J. M. Millam, M. Klene, J. E. Knox, J. B. Cross, V. Bakken, C. Adamo, J. Jaramillo, R. Gomperts, R. E. Stratmann, O. Yazyev, A. J. Austin, R. Cammi, C. Pomelli, J. W. Ochterski, R. L. Martin, K. Morokuma, V. G. Zakrzewski, G. A. Voth, P. Salvador, J. J. Dannenberg, S. Dapprich, A. D. Daniels, O. Farkas, J. B. Foresman, J. V. Ortiz, J. Cioslowski, D. J. Fox, *Gaussian*, Inc., Wallingford CT, 2013.
7. P. Politzer, Y. Ma, P. Lane, M. C. Concha, *Int J Quant Chem*, **105**, 341-347 (2005).
8. T. Lu, F. Chen, *J Comput Chem*, **3**, 580–592 (2012).
9. A. Devi, S. Dharavath, V. D. Ghule, *ChemistrySelect.*, **3**, 4501–4504 (2018).
10. H. D. B. Jenkins, D. Tudela, L. Glasser, Lattice Potential Energy Estimation for Complex Ionic Salts from Density Measurements, *Inorg. Chem.*, **41**, 2364 (2002).